

AD-A049 220

UNCLASSIFIED

| OF |
AD
A049220

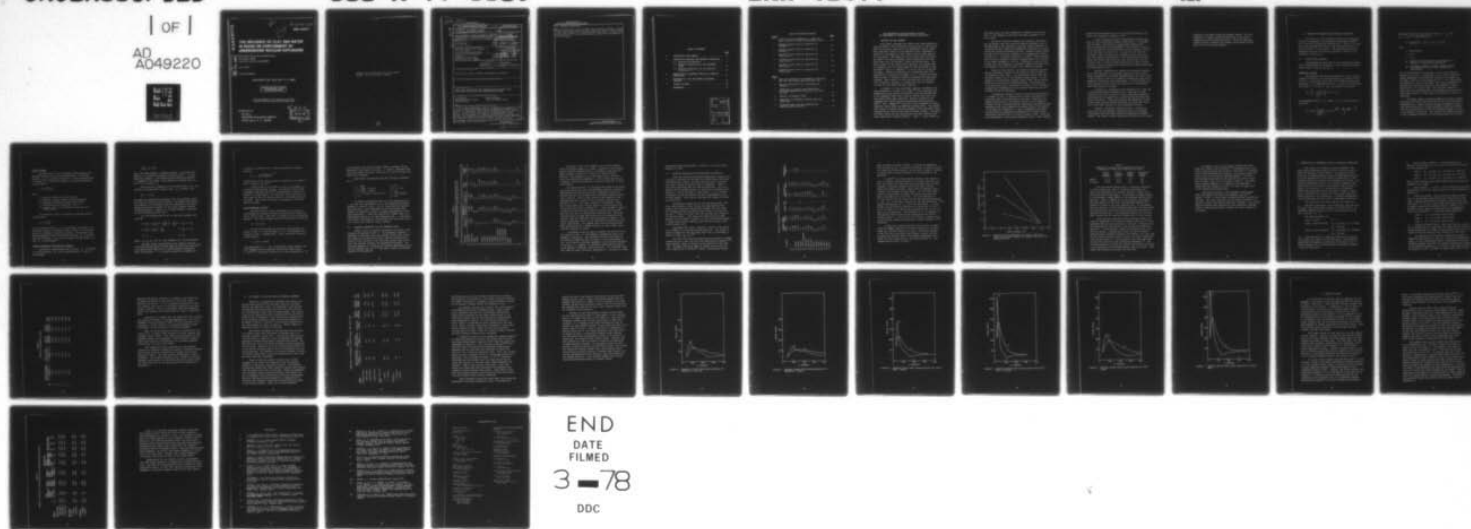


SYSTEMS SCIENCE AND SOFTWARE LA JOLLA CALIF
THE INFLUENCE OF CLAY AND WATER IN ROCKS ON CONTAINMENT OF UNDE--ETC(U)
JUN 77 N RIMER

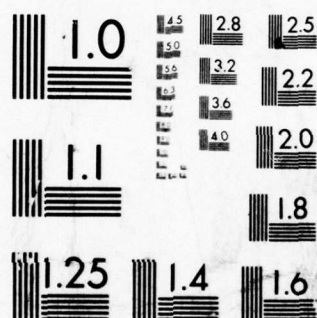
SSS-R-77-3339

DNA-4347T

F/G 18/3
DNA001-77-C-0099
MI



END
DATE
FILMED
3-78
DDC



MICROCOPY RESOLUTION TEST CHART
NATIONAL BUREAU OF STANDARDS-1963-A

AD A 0 4 9 2 2 0

DDC FILE COPY

2

12

AD-E 300 034

DNA 4347T

THE INFLUENCE OF CLAY AND WATER IN ROCKS ON CONTAINMENT OF UNDERGROUND NUCLEAR EXPLOSIONS

Systems, Science and Software
P.O. Box 1620
La Jolla, California 92038

June 1977

Topical Report

CONTRACT NO. DNA 001-77-C-0099

APPROVED FOR PUBLIC RELEASE;
DISTRIBUTION UNLIMITED.

THIS WORK SPONSORED BY THE DEFENSE NUCLEAR AGENCY
UNDER RDT&E RMSS CODE B345077462 J24AAXYX98349 H2590D.

Prepared for
Director
DEFENSE NUCLEAR AGENCY
Washington, D. C. 20305

DDC
RECEIVED
JAN 27 1978
RECEIVED
A

Destroy this report when it is no longer
needed. Do not return to sender.



DNA, SBIE

UNCLASSIFIED

SECURITY CLASSIFICATION OF THIS PAGE (When Data Entered)

19 REPORT DOCUMENTATION PAGE		READ INSTRUCTIONS BEFORE COMPLETING FORM
1. REPORT NUMBER	2. GOVT ACCESSION NO.	3. RECIPIENT'S CATALOG NUMBER
DNA 4347T, AD-E300 034		9
4. TITLE (and Subtitle)	5. TYPE OF REPORT & PERIOD COVERED	
THE INFLUENCE OF CLAY AND WATER IN ROCKS ON CONTAINMENT OF UNDERGROUND NUCLEAR EXPLOSIONS	Topical Report.	
7. AUTHOR(s)	14. PERFORMING ORG. REPORT NUMBER	8. CONTRACT OR GRANT NUMBER(s)
Norton Rimer	SSS-R-77-3339	
9. PERFORMING ORGANIZATION NAME AND ADDRESS	10. PROGRAM ELEMENT, PROJECT, TASK AREA & WORK UNIT NUMBERS	
Systems, Science and Software P.O. Box 1620 La Jolla, California 92038	Subtask J24AAXYX983-49	
11. CONTROLLING OFFICE NAME AND ADDRESS	12. REPORT DATE	13. NUMBER OF PAGES
Director Defense Nuclear Agency Washington, D.C. 20305	June 1977	44
14. MONITORING AGENCY NAME & ADDRESS (if different from Controlling Office)	15. SECURITY CLASS (of this report)	15a. DECLASSIFICATION DOWNGRADING SCHEDULE
1243 P.	UNCLASSIFIED	
16. DISTRIBUTION STATEMENT (of this Report)		
Approved for public release; distribution unlimited.		
17. DISTRIBUTION STATEMENT (of the abstract entered in Block 20, if different from Report)		
18. SUPPLEMENTARY NOTES		
This work sponsored by the Defense Nuclear Agency under RDT&E RMSS Code B345077462 J24AAXYX98349 H2590D.		
19. KEY WORDS (Continue on reverse side if necessary and identify by block number)		
Containment Residual Stress Fields Ground Motion Shear Strength Clay and Water Content		
20. ABSTRACT (Continue on reverse side if necessary and identify by block number)		
This report describes a series of spherically symmetric calculations of the ground motions due to underground nuclear tests located in Nevada Test Site rocks of different clay and water contents. In particular, calculations of the Baneberry event, believed to be located in a rock of unusually high clay and water content, are compared with calculations for more typical NTS rocks. The Baneberry medium is thought to have considerably lower		

DD FORM 1 JAN 73 1473 EDITION OF 1 NOV 65 IS OBSOLETE

UNCLASSIFIED

SECURITY CLASSIFICATION OF THIS PAGE (When Data Entered)

388 507

UNCLASSIFIED

SECURITY CLASSIFICATION OF THIS PAGE(When Data Entered)

20. ABSTRACT (Continued)

shear strength due to the abnormal clay and water contents. Calculations with these lower strengths showed far lower residual stress fields when compared to calculations for other media. A discussion of the relevance of these calculational results to containment is presented. ←

UNCLASSIFIED

SECURITY CLASSIFICATION OF THIS PAGE(When Data Entered)

TABLE OF CONTENTS

	<u>Page</u>
1. INTRODUCTION AND SUMMARY.	3
2. CONSTITUTIVE MODELING AND MATERIAL PROPERTIES . .	7
2.1 Constitutive Modeling.	7
2.2 Material Properties for the Parameter Study.	12
2.3 Material Properties for Calculations of Section 4	15
3. SENSITIVITY OF BANEERRY RESULTS TO MODELING ASSUMPTIONS	21
4. THE EFFECT OF CLAY AND WATER ON RESIDUAL STRESSES.	25
5. FIGURES OF MERIT.	35
REFERENCES.	39

ACCESSION FOR	
NTIS	White Section <input checked="" type="checkbox"/>
DOC	Buff Section <input type="checkbox"/>
UNANNOUNCED	<input type="checkbox"/>
JUSTIFICATION	
BY	
DISTRIBUTION/AVAILABILITY CODES	
Dist.	AVAIL. NO. or SPECIAL
A	

LIST OF FIGURES AND TABLES

<u>Figure</u>		<u>Page</u>
1	Uniaxial stress difference at 4 kbars vs. water content for Terra Tek laboratory data. . . .	18
2	Residual stress field vs. position for Baneberry 1.	29
3	Residual stress field vs. position for Baneberry 2.	30
4	Residual stress field vs. position for Yucca Flat 1	31
5	Residual stress field vs. position for Yucca Flat 2	32
6	Residual stress field vs. position for Dido Queen	33
7	Residual stress field vs. position for Mighty Epic.	34

<u>Table</u>		
1	Material properties for Baneberry, Yucca Flat dry tuff and Rainier Mesa saturated tuff	13
2	Material properties for calculations of Section 4.	16
3	Comparison of results using TAMEOS and Tillotson equations of state for Yucca Flat dry tuff	19
4	Results of parameter study	23
5	Comparison of Baneberry, Rainier Mesa and Yucca Flat	26
6	Figures of merit for equilibrated and unequilibrated cavities.	37

THE INFLUENCE OF CLAY AND WATER IN ROCKS
ON CONTAINMENT OF UNDERGROUND NUCLEAR EXPLOSIONS

1. INTRODUCTION AND SUMMARY

This report discusses the effects that large amounts of clay and water in the surrounding rock may have on the containment of hot cavity gases due to an underground nuclear event. The containment failure of the Baneberry event, detonated in Yucca Flat in December of 1970, seems to be an ideal vehicle for this study. The Baneberry site has been characterized by the USGS^[1] as having unusually high concentrations of montmorillonite clay (65 percent) around the working point. The water content of the working point material (an altered tuff) is related to the clay content and has been estimated by both the USGS^[1] and by L. Ramspott^[2] to be as much as 25 percent by weight. Material properties data for Rainier Mesa tuff, compiled by S. Butters of TerraTek, Inc.^[3] indicate that high water content in laboratory samples correlates with low shear strength. While there is little hard data on the effect of clay on material strength, it seems clear that the presence of clay can only weaken the host material.

A scenario for the containment failure of Baneberry has been presented in a report by N. Rimer^[4] which discusses one-dimensional ground motion calculations using the SKIPPER code of the Baneberry event and of typical Rainier Mesa and Yucca Flat events which were contained. Material properties for Baneberry were based on site investigations and analyses by USGS^[1] and L. Ramspott^[2] which led to the assumption of three spherical layers about the Baneberry working point. The working point layer of altered tuff was assumed to have negligible shear strength due to the very high clay and water content. The second and third layers for the calculations were both alluvium (the third layer was of infinite extent). Since the clay content of

the second layer had been estimated at between 20 and 50 percent, it was assumed to have half the shear strength of the third layer.

The major difference between the Baneberry calculation and the Rainier Mesa and Yucca Flat results appeared to be in the magnitude of the compressive residual stress fields due to nonuniform plastic loading and subsequent unloading of the rock around the explosion-produced cavities. Residual stress fields are seen after the cavity rebounds in all ground motion calculations at S^3 . Parameter studies by N. Rimer^[5] have indicated that the peak transverse residual stresses depend very strongly on the shear strength of the rock. Therefore, it was not surprising that the Baneberry calculation, modeled with relatively low strength, gave significantly lower residual stresses.

Based on these results, the following scenario was presented as possibly leading to the venting of cavity gases to the surface at late times. The low strength due to high clay and water content led to low residual stress fields. In the absence of a significant residual stress field, the hot cavity gases could cause tensile hydrofracturing. The fracturing, if sufficiently great, could lead to venting. The low material strength was considered to be the primary reason for the containment failure of Baneberry.

Although the original report of this work was written in the summer of 1975, it received only limited distribution to interested ERDA representatives at the time. Because of the general sensitivity of the subject matter, we were asked to withhold further distribution until additional calculations were completed which would determine the sensitivity of the results to the modeling assumptions. A set of suggested multi-layer calculations was completed and presented at an Earth Motion Calculators meeting held in La Jolla on May 4, 1976. Since the multi-dimensional calculations requested in Ref. 4 have recently

been done and presented by LLL at the 66th CEP meeting, the report was released in January of 1977.

In the intervening period, considerable work has been done to clarify questions raised by that report. The present work includes a discussion of constitutive modeling and material properties data improvements (see Section 2) used in later calculations of both Baneberry and the comparison events in Rainier Mesa and Yucca Flat. It was felt that the comparisons in Ref. 4 might not be completely valid since there were some modeling differences in the calculations being compared (the Rainier Mesa and Yucca Flat calculations, as described in Ref. 4, were not made specifically as part of this program.) Careful consideration has shown that those comparisons are qualitatively valid.

Section 3 describes the results of calculations presented at the Earth Motion Calculators meeting of May 4, 1976. Based on suggestions from ERDA representatives, the sensitivity of the results to some of the modeling assumptions used in the Baneberry calculation was investigated. It was found that the basic results of Ref. 4 were not sensitive to any parameter other than material strength.

In Section 4, calculations are presented for a weak and a strong Rainier Mesa saturated tuff, a weak and a strong Yucca Flat dry tuff, as well as a weak, best-guess Baneberry calculation and an upper-limit, relatively-high-strength Baneberry calculation. These calculations show Baneberry to have a much lower residual stress field than the other NTS events due to the lower strength of the surrounding alluvium.

Section 5 discusses "figures of merit," measures by which one can tell whether a particular event is a greater containment risk than other previously-detonated successful events. The figure of merit chosen was the ratio of the cavity

pressure to the peak transverse residual stress. For this comparison, a sophisticated determination of the cavity pressure was used as described below. Using the resulting figure of merit, Baneberry was clearly the greatest containment risk of the events examined.

2. CONSTITUTIVE MODELING AND MATERIAL PROPERTIES

In Section 2.1, the constitutive models are discussed briefly with emphasis on the modeling improvements between Ref. 4 and the calculations presented here. Section 2.2 gives the material properties used for the calculations of Ref. 4 and of Section 3 of this report. The modeling and material properties used for the results presented in Section 4 are discussed in Section 2.3.

2.1 CONSTITUTIVE MODELING

Descriptions are given here of the constitutive models used in the SKIPPER calculations. A more complete discussion may be found in Cherry, et. al.^[6]

Equations of State

The Baneberry calculations described in Ref. 4 used an equation of state of the form developed by Tillotson^[7] and fit at S^3 to available shock data for a number of geological materials. For compressed states ($\rho > \rho_0$) and for cold expanded states ($\rho < \rho_0$ and $e < e_s$), the pressure is given by

$$P_s = \left[a + \frac{b}{\frac{e}{e_0 \eta^2} + 1} \right] e \rho + A \mu + B \mu^2 \quad .$$

For expanded states ($\rho < \rho_0$) where $e > e_s$, the pressure is given by

$$P_v = a e \rho + \left[\frac{b e \rho}{\frac{e}{e_0 \eta^2} + 1} + A \mu e^{-\beta \left(\frac{\rho_0}{\rho} - 1 \right)} \right] e^{-\bar{\alpha} \left(\frac{\rho_0}{\rho} - 1 \right)^2} \quad .$$

The phase transition from liquid to vapor ($\rho < \rho_0$ and $e_s < e < e'_s$) is approximated as

$$P = \frac{1}{e'_s - e_s} \left[(e - e_s) P_v + (e'_s - e) P_s \right] .$$

Here

ρ = mass density

$\eta = \rho/\rho_0$

$\mu = \eta + 1$

e_s = specific internal energy as the material is brought to vaporization temperature

e'_s = additional specific internal energy required to change the material from a liquid to a vapor state

All the above formulas assume that no air-filled voids are present in the rock. The constants, a , b , and e_0 govern the energy dependence of the material, allowing it to behave as an ideal, γ -law gas at high energies ($a \sim \gamma - 1$), and reducing the effective γ at lower energies. The density dependence is governed by a quadratic polynomial with constants A and B which may be fit to shock data. The Tillotson equation of state does not accurately model the expansion from rock states above approximately 10 kbars where the expansion of steam is important.

The Tabular Array of Mixtures Equation of State (TAMEOS) described in Cherry^[6] has been used for all tuff calculations discussed here. TAMEOS mixes the proper percentage of water with grain density rock, assuming pressure equilibrium between the rock and the water, to give the pressure response for the fully crushed tuff mixture. This gives a far better description of the subsequent expansion of the shocked water-rock mixture.

Porous Crushup

The equations of state discussed above describe the pressure response for fully saturated rocks. Air-filled porosity ϕ_0 is included through the S^3 porous crushup model (P- α model) [6] in which the pressure of the porous material is described by

$$P = \frac{1}{\alpha} \bar{P} \left(\frac{V}{\alpha}, e \right)$$

where

V = specific volume of porous material

e = specific internal energy of porous material

\bar{P} = pressure obtained from equation of state

α = distension ratio defined by $V/\bar{V} \geq 1$

\bar{V} = specific value of the material with zero air-filled voids

The distension ratio is required to decrease from an initial value

$$\alpha_0 = \frac{1}{1 - \phi_0}$$

at zero pressure down to 1.0 as the pressure increases to P_c , the crush pressure or pressure limit at which all air-filled porosity is assumed irreversibly removed. Any porosity lost during compression below the elastic pressure P_e is recoverable upon expansion. Any porous crushup occurring between P_e and P_c is irreversible.

Elastic Properties and Material Strength

The ambient compressional wave velocity C_0 is related to the bulk modulus K_0 and the shear modulus G by the relationship

$$\rho_0 C_0^2 = K_0 + \frac{4}{3} G$$

Here, the shear modulus is assumed constant. Since the bulk modulus K varies with pressure, Poisson's ratio σ is not being held constant. One calculation was made with constant σ throughout the crushup. This requires a constant ratio of K/G , i.e., a varying G .

The deviatoric components of the stress tensor S_{ij} are related to the deviatoric strain rates $\dot{\epsilon}_{ij}$ by Hooke's law

$$\dot{S}_{ij} = 2 G \dot{\epsilon}_{ij}$$

The material strength model requires that the principal stress be within the von Mises yield surface. For spherical geometry, this reduces to the condition that the magnitude of the radial deviatoric stress not exceed 2/3 the yield strength (maximum stress difference). Behavior of a failed element is governed by the non-associated flow rule.

For the calculations of Ref. 4, the yield strength was given by

$$Y = \left[Y_0 + Y_m \frac{P}{P_m} \left(2 - \frac{P}{P_m} \right) \right] \left(1 - \frac{e}{e_m} \right) \quad P < P_m, e < e_m$$

$$Y = \left(Y_0 + Y_m \right) \left(1 - \frac{e}{e_m} \right) \quad P \geq P_m, e < e_m$$

$$Y = 0 \quad , \quad e > e_m$$

where Y_0 , Y_m , P_m and e_m are constants for a given material.

The more recent calculations use an improved form for the yield strength which has been shown by Cherry and Peterson^[8] to be empirically superior to a simple pressure dependence. Here, the pressure P in the above equations is replaced by

\bar{P} which is a function of P and the deviatoric stresses given by

$$\bar{P} = P - \frac{1}{2} \left(\frac{S_{11}S_{22}S_{33}}{2} \right)^{1/3}$$

A description of how shear failure is treated in this model is given in Cherry, et. al.^[6]

Tension failure is allowed to occur in an element if a principal stress becomes tensile. The tension failure model proposed by Maenchen and Sack^[9] and described in detail by Cherry^[6] is then applied. An inelastic strain which is just sufficient to zero the tensile stress is introduced normal to the crack. This strain increases or decreases as the crack opens or closes.

Cavity Equation of State

The cavity source region was chosen to be initially large enough to vaporize 70 metric tons of rock for each kiloton of device yield. (The rock is assumed to be at undisturbed density.) The cavity pressure for all calculations is given by

$$P = (\gamma - 1) e/V$$

For the Rainier Mesa and Yucca Flat calculations described in Ref. 4, γ was set equal to 1.5. The Baneberry calculation of Ref. 4 assumed that γ was a function of specific volume given by

$$\gamma = 1.03 + 0.9/\sqrt{V}$$

This expression for γ was a preliminary result obtained for tuff modeled using the chemical equilibrium CHEST code of D. Laird^[10] and has been modified for later calculations. It

will be shown later that the peak residual stresses are not sensitive to the choice of cavity γ . However, depending upon the cavity model used, peak velocities at a given location may differ by 20 percent.

More recent calculations used the following expression for γ .

$$\begin{array}{ll} \gamma' = 1.085 & V \geq 1.9 \\ \gamma' = 1.2085 - 0.065 V & 1.9 > V \geq 0.9 \\ \gamma' = 1.9375 - 0.875 V & V < 0.9 \\ \gamma = \gamma' - 0.032 + 3.2 \times 10^{-13} e & e > 10^{11} \text{ ergs/gm} \\ \gamma = \gamma' & e \leq 10^{11} \end{array}$$

It should be emphasized that the above expressions for γ are only very approximate fits to the complicated tabular equation of state of Laird. The fit given above was derived from data from a table developed for one particular water content (24 percent by weight, including approximately 7 percent bound water). Since the creation of a CHEST table is a complicated procedure, the same expression for γ was used in calculations for Baneberry, Rainier Mesa and Yucca Flat tuffs, i.e., over a wide range of water contents.

2.2 MATERIAL PROPERTIES FOR THE PARAMETER STUDY

Table 1 gives the material properties data used in the original calculations of Ref. 4. For Baneberry, Material 1 describes a saturated, high clay content altered tuff extending radially 15.24 meters (50 feet) from the working point. Since the clay content of this layer was greater than 50 percent, the material strength was considered negligible. The Tillotson equation of state, using constants approximating the data of Stephens, et. al.,^[11] was used to model the pressure response of the material.

Table 1
Material properties for Baneberry, Yucca Flat dry tuff
and Rainier Mesa saturated tuff (Reproduced from Ref. 4)

Property	Baneberry			Yucca Flat	Rainier Mesa
	Material 1	Material 2	Material 3		
ρ_o (gm/cm ³)	1.91	2.128	2.016	1.7	1.91
c_o (km/sec)	1.607	2.086	1.606	2.13	2.34
G (kbar)	7	30	15	25.8	35.7
k_o (kbar)	40	50	32	55	57.2
ϕ_o	0	0.05	0.10	0.1564	0.012
Y_m (kbar)	0	0.05	0.10	0.62	0.18
Y_o (kbar)	0	0.007	0.007	0.12	0.055
P_m (kbar)	0	0.7	0.7	0.4	0.4
P_e (kbar)	--	0.07	0.07	0.18	0.05
P_c (kbar)	--	2.0	2.0	4.36	1.5
P_o (kbar)	0.060	0.060	0.060	0.096	0.056
e_m (10 ¹⁰ erg/gm)	2.15	2.15	2.15	2.0	2.0
e_s (10 ¹⁰ erg/gm)	3.7	3.7	3.7	--	--
e'_s (10 ¹⁰ erg/gm)	17.5	17.5	17.5	--	--
e_o (10 ¹⁰ erg/gm)	10	10	10	--	--
A (kbar)	40	79.3	79.3	--	--
B (kbar)	352	803	803	--	--
a	0.4	0.4	0.4	--	--
b	0.6	0.6	0.6	--	--
f	--	--	--	0.136	0.17
$\frac{f_w}{\alpha}$	5	5	5	--	--
β	5	5	5	--	--

Materials 2 and 3 are assumed to be alluvium modeled using a Tillotson equation of state. Material 2, with greater than 20 percent montmorillonite, is assumed to have half the shear strength of Material 3, which is a weak alluvium. Material 2 was assumed to be 36.58 meters thick (120 feet) and to be surrounded by Material 3. Free surface effects and a radially varying gravitational field were neglected in these calculations.

The measured data^[1,2] upon which the modeling was based was often conflicting since the Baneberry geology is unusually complicated and since the data were accumulated from holes drilled both pre and postshot and in different locations relative to the WP. The log data indicated that Material 2 had a compressional wave velocity 20 to 30 percent greater than Materials 1 or 3. This was included in the modeling. Also, due to the higher clay content, Material 2 had only half the air-filled void content of Material 3. Also included in Table 1 is material properties data used for calculations for Yucca Flat dry tuff and for Rainier Mesa saturated tuff. These calculations were not made specifically for the Baneberry study but were used for comparison with the Baneberry results. As a result, differences exist in the constitutive modeling for the three calculations. For example, both Yucca Flat and Rainier Mesa calculations use a TAMEOS equation of state rather than a Tillotson equation of state.

A parameter study was made to examine the sensitivity of the results of Ref. 4 to the modeling assumptions used in the Baneberry calculation. The starting point for this study is the material properties data of Table 1. The calculations of Ref. 4 all used the pressure dependent failure surface described in Section 2.1. However, the parameter study used the empirically superior \bar{P} dependent failure surface. The parameter study also used the newer functional dependence of γ on specific volume

and energy which was described in Section 2.1 for the cavity equation of state.

2.3 MATERIAL PROPERTIES FOR CALCULATIONS OF SECTION 4

Using the constitutive modeling described in Section 2.1, a series of calculations was made for Rainier Mesa (Dido Queen and Mighty Epic events), for Yucca Flat dry tuff (a calculation using average properties) and for Baneberry. Table 2 gives the properties used for these calculations. All calculations use the TAMEOS equation of state for the working point material, a cavity equation of state where γ is a function of specific volume and energy, and the \bar{P} dependence for the failure surface. This section discusses the properties chosen for each event.

The material properties for the Dido Queen event, density, grain density, water content and compressional wave velocity were obtained from the CEP document for that event. The failure envelope was modeled using Figure 24 of Butters, et. al. [12] while the crush curve was obtained from Figure 19 of the same report. Dido Queen was chosen for this study because it was located in tunnel e of the Rainier Mesa complex, a tunnel that triaxial loading tests indicate contains relatively weaker tuffs.

The Mighty Epic event, located in tunnel n, was chosen as an example of a stronger Rainier Mesa tuff. The choice of material properties for the Mighty Epic event is discussed in detail in Rimer, et. al. [13]

The Yucca Flat material properties were based on average properties for a Yucca Flat dry tuff summarized by Ramspott. [14] Unfortunately, there is no data on the strength of this material. TerraTek laboratory data for Rainier Mesa tunnel bed tuffs compiled by S. Butters [3] shows a relationship between

Table 2
Material properties for Calculations of Section 4

Property	Rainier Mesa		Yucca Flat 1	Baneberry 1		Baneberry 2 Layer 2
	Dido Queen	Mighty Epic		Layer 1	Layer 2	
f_w	0.16	0.17	0.13	0.22	0.10	--
ϕ_o	0.016	0.02	0.16	0	0.07	--
Y_o (kbar)	0.065	0.072	0.1	0.03	0.08	0.05
Y_m (kbar)	0.335	0.628	0.53	0.05	0.14	0.09
P_m (kbar)	3.0	1.0	3.0	2.0	2.0	--
e_m (10 ¹⁰ ergs/gm)	2.0	2.0	2.0	2.15	2.15	--
ρ_o (gm/cm ³)	1.92	1.93	1.7	2.00	2.11	--
ρ_G (gm/cm ³)	2.383	2.46	2.39	2.786	2.64	--
C_o (km/sec)	2.48	2.64	1.8	1.554	1.8	--
G (kbar)	35.8	53	18.8	10.7	24.5	--
K_o (kbar)	70	64	30	34	38	--
P_e (kbar)	0.1	0.1	0.1	--	0.1	--
P_c (kbar)	3.5	4.0	4.0	--	4.0	--
P_o (kbar)	0.075	0.075	0.060	0.060	0.060	--
A (kbar)	--	--	--	--	52.4	--
B (kbar)	--	--	--	--	1416	--

shear strength and water content. It should be emphasized that the data of Ref. 3 is stress difference in uniaxial strain at 4 kbars confining pressure, not the yield strength. However, it should give a relative indicator of the strength of the materials.

F. App^[15] has drawn several straight lines through a plot of strength (stress difference of 4 kbars) vs water content (by weight) for these data which indicate that the shear strength is inversely proportional to the water content. These lines shown in Figure 1 imply that for Baneberry water contents, the strength is quite small. For the lower water content of Yucca Flat tuff above the water table, the plot gave a strength value of 0.63 kb. The yield strength of 0.63 for Yucca Flat tuff water content was apportioned between Y_o and Y_m in the ratio suggested by the Dido Queen data. This leaves the magnitude of P_m yet to be determined. For this reason, two calculations were made for Yucca Flat, one for a P_m of 3.0 kbar, as in Dido Queen, and another for a P_m of 1.0 kbar, as in Mighty Epic. The parameter P_m is as important to the residual stress field as the magnitude of the failure strength itself. A low value of P_m indicates a steeper slope of the failure surface and therefore a higher strength at low pressures.

A Yucca Flat calculation made with the data of Table 2 using the TAMEOS equation of state was compared to one made using the Tillotson equation of state. Tillotson constants A and B for this calculation were chosen to match the zero pressure bulk modulus used in the TAMEOS calculation and to match its zero energy curve at the crush pressure P_c . The comparisons are given in Table 3.

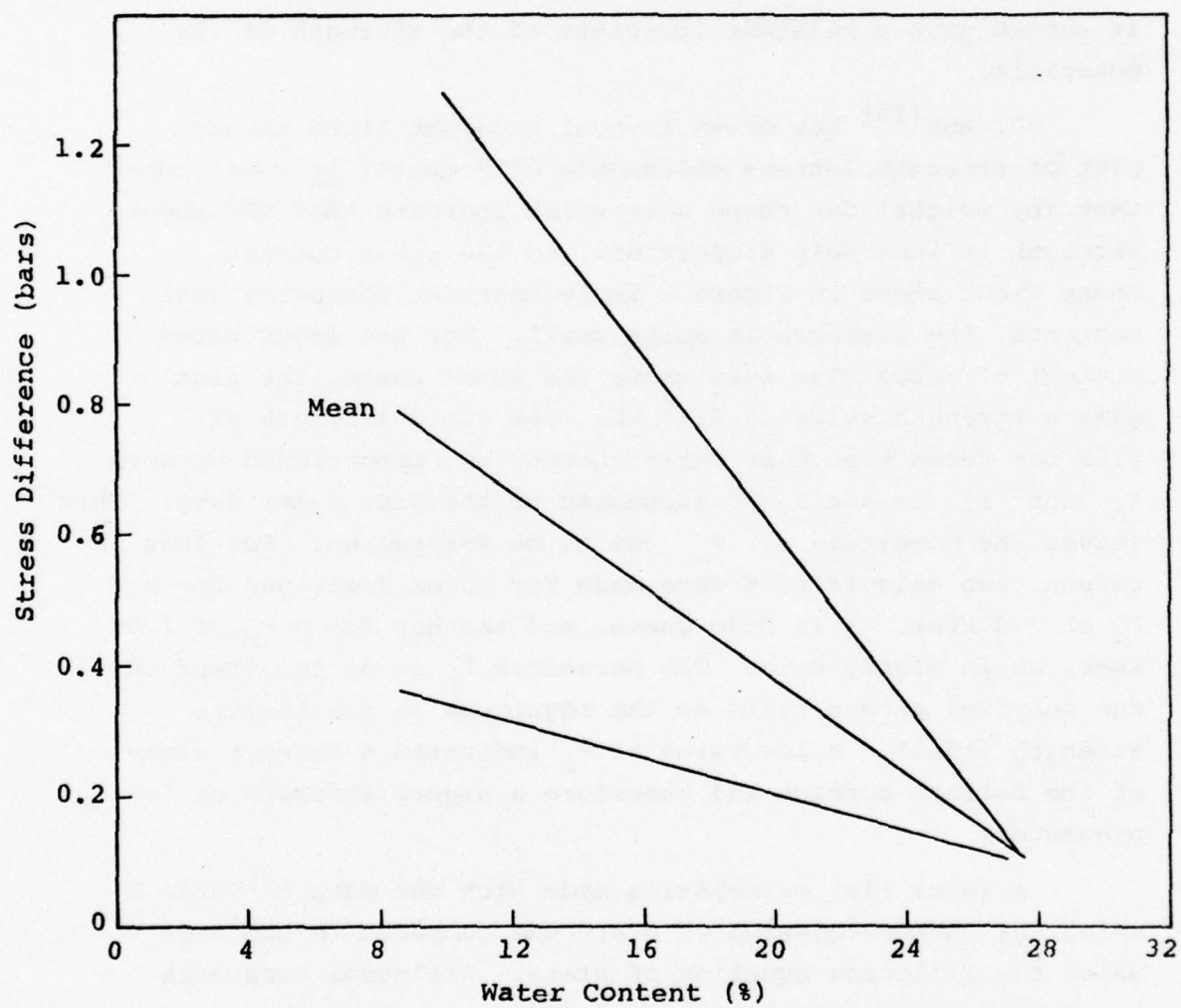


Figure 1. Uniaxial stress difference at 4 kbars (range and mean) versus water content (by weight) for Terra Tek laboratory data.

Table 3
Comparison of results using TAMEOS and Tillotson
equations of state for Yucca Flat dry tuff

	Cavity radius (meters)	Cavity pressure (bars)	Radial stress (bars)	Transverse stress (bars)
TAMEOS	31.70	136.7	174	304
Tillotson	29.18	183.9	140	249

The calculations showed about a 10 percent difference in cavity radius and close to 20 percent differences in radial and transverse peak residual stresses. Cavity pressures were even further apart. On the basis of these results, it was decided to apply TAMEOS to the Baneberry working point material. Input to TAMEOS is the water content (by weight), the grain density of the tuff, and constants defining the equation of state of the grain density tuff. It was assumed that the equation of state constants applicable to Rainier Mesa tuff (having much lower grain densities) may be used for the Baneberry altered tuff. The important features are the high water content and the high grain density due to clay content.

Since the peak residual stresses had been shown to be primarily dependent on the failure strength and not to be very dependent upon the exact position of the layer interface or on the compressional wave velocity (the results are presented in Section 3), it was decided to model the Baneberry site using only two layers, a working point layer of over 50 percent montmorillonite extending radially 35.66 meters (117 feet) from the WP, with an alluvium layer of lower, but still significant clay content around it. The location of the layer was based on data from drill hole Ue8i discussed by Ramspott.^[2] The Tillotson equation of state was used for the second layer which is not expected to see stresses greater than 5-10 kbars. Both layers were modeled using data from hole Ue8i.

For layer 2, data on the failure envelope has been found for Diagonal Line alluvium,^[16] considered to be a relatively strong alluvium and for Merlin alluvium,^[17] considered to be a more representative alluvium. The strength given for layer 2 for the calculation labeled Baneberry 1 in Table 2 was obtained using Diagonal Line alluvium data and so represents an upper limit to the strength of layer 2. The calculation labeled Baneberry 2 is identical with Baneberry 1 except that the strength of layer 2 is lower as shown since it was modeled using Merlin data.

The failure strength of the Baneberry working point layer was modeled using data from Stephens, et. al.^[11] Figure 7 of Ref. 17 plots shear strength vs water contents for alluvium. That plot indicates that for water contents of 20 percent or more, alluvium has zero shear strength. This implies that the working point material may have negligible strength. Figure 1 indicates negligible strength for water contents of 30 percent.

3. SENSITIVITY OF BANEERRY RESULTS TO MODELING ASSUMPTIONS

The results of a parameter study presented at the Earth Motion Calculators meeting held in La Jolla on May 4, 1976 are discussed in this section. The purpose of this study was to answer questions raised by ERDA representatives as to the sensitivity of the results of Reference 4 to the modeling assumptions used for the Baneberry calculation. The material properties used for the 3 material Baneberry base calculation are those used for Reference 4 and are given in Table 1 of Section 2.2. A second look at the modeling assumptions indicated that the thickness of layer 2 (material 2) should be 51.8 meters (170 feet) rather than 36.58 meters (120 feet) as in Reference 4. Modeling improvements were incorporated into this study as described in Section 2.

The calculations of this study are the following:

1. The base calculation: This calculation uses the data of Table 1 but assumes that layer 2 is 170 feet thick. An important feature is that the cavity gas equation of state has a constant γ of 1.5.

The yield strengths are

Layer 1 (clay) $Y = 0$

Layer 2 (half strength) $Y_o = 7.0$ bars, $Y_m = 50$ bars,
 $P_m = 700$ bars

Layer 3 (full strength) $Y_o = 7.0$ bars, $Y_m = 100$ bars,
 $P_m = 700$ bars

- 1a. This calculation is identical with the base calculation except that layer 2 is 120 feet thick. It essentially duplicates the Baneberry calculation of Reference 4 with better modeling for the failure surface and with a constant γ for the cavity gas.

2. High strength, constant γ : This calculation is identical with calculation (1) except for material strengths. The new strengths are

Layer 1 $Y_o = 30$ bars, $Y_m = 10$ bars, $P_m = 700$ bars
Layer 2 $Y_o = 30$ bars, $Y_m = 50$ bars, $P_m = 700$ bars
Layer 3 $Y_o = 30$ bars, $Y_m = 100$ bars, $P_m = 700$ bars

The WP layer has been given some strength and Y_o has been increased in all layers.

3. High strength, $\gamma = g(V,e)$: This calculation duplicates calculation (2) with the cavity equation of state described in Section 2.1.

4. High sound speed: This calculation repeats calculation (3) with higher compressional wave velocities in each layer. The new sound speeds correspond closer to logs from hole U8a10.^[1] To reach these higher velocities, each layer is given a larger bulk and shear modulus. However, its Poisson's ratio remains the same as for the corresponding layer of calculation (3). The higher sound speeds are

Layer 1 $C_o = 2.03$ km/sec (6700 ft/sec)
Layer 2 $C_o = 2.41$ km/sec (7900 ft/sec)
Layer 3 $C_o = 2.0$ km/sec (6600 ft/sec)

5. Constant Poisson's ratio: This calculation is identical to calculation (3) except that the shear modulus for each calculational zone is allowed to vary during porous crushup in order to maintain Poisson's ratio constant for that zone.

The results of this study are summarized in Table 4. Comparing calculations (1) and (1a), clearly the thickness of layer 2 is not a significant factor in magnitude of the peak residual stresses (note that all residual stresses are relative to an overburden pressure P_o of 60 bars), final cavity radius or pressure, or RDP. The RDP (or steady state value of the

Table 4
Results of Parameter Study

ID	Peak Transverse Residual Stress (bars)	Peak Radial Residual Stress (bars)	Cavity Radius (meters)	Cavity Pressure (bars)	RDP (m ³)
1	21.6	5.5	43.96	19.5	7350
1a	22.4	7.6	44.68	19.7	7600
2	62.2	25.2	44.57	18.3	7250
3	77.7	40.0	43.72	41.5	7800
4	73.2	35.9	43.77	41.4	7000
5	78.4	32.2	43.48	42.3	9800

reduced displacement potential) is defined as the final displacement multiplied by the square of the initial radial distance from the WP. It is a constant with position in the far (elastic) field and is a qualitative measure of the teleseismic coupling. It will be discussed later when Baneberry results are compared with calculations of events in other NTS media.

Calculation (2) shows that, for higher material strength, the residual stresses are increased dramatically. This is in agreement with the results of Rimer,^[5] which indicate that increasing Y_0 is most effective in increasing residual stress magnitudes. Cavity pressure is relatively unchanged.

When the cavity equation of state is altered as in calculation (3), a larger cavity pressure is noted, together with a smaller cavity radius. This larger cavity pressure is still somewhat smaller than overburden. Modifications in compressional wave velocity (calculation 4) or in elastic behavior (calculation (5)) have little effect.

This sensitivity study indicates that the residual stresses are primarily affected by changes in material strength while cavity pressure is modified by changes in the cavity equation of state. The basic results of Reference 4 remain unchanged. The residual stresses, while larger for the high strength calculations, are still much smaller than the results for Yucca Flat tuff and for Rainier Mesa tuff presented in Reference 4.

4. THE EFFECT OF CLAY AND WATER ON RESIDUAL STRESSES

Spherical, one-dimensional SKIPPER calculations for a working point medium having extremely high clay and water content (the Baneberry event) are discussed in this section and compared with calculations for Yucca Flat dry tuff and for the saturated tunnel tuffs of Rainier Mesa. All calculations use the same constitutive modeling and the same device yield so that differences in the results are a function only of the material properties chosen (constitutive models are discussed in detail in Section 2 and material properties for the calculations are given in Table 2). Table 5 shows the important results of these calculations.

The events considered for Rainier Mesa are Dido Queen in a weaker tunnel tuff environment and Mighty Epic in a stronger, atypical tunnel tuff. A second Dido Queen calculation was made for comparison using the Baneberry overburden pressure of 60 bars which barely perturbed the results. The Yucca Flat dry tuff calculations represent average properties for that area. These two Yucca Flat calculations differ only in the failure envelope used as do the two Baneberry calculations presented. All Baneberry calculations assumed 2 layers; one having greater than 50 percent montmorillonite clay, and the other less than 50 percent.

Table 5 gives the maximum values of the residual stresses in the radial and transverse (hoop) directions relative to the scalar overburden pressure. The Baneberry calculations showed much lower residual stresses when compared with the other Yucca Flat calculations. While the comparison with the weaker Rainier Mesa calculations (Dido Queen) was not as dramatic, the calculations still differ considerably. The most important material properties in determining the values of the residual stresses are the magnitude and shape of the failure surface. Since the "strong" Baneberry

Table 5
Comparison of Baneberry, Rainier Mesa, and Yucca Flat

Event	Peak Transverse Residual Stress (bars)	Peak Radial Residual Stress (bars)	Overburden (bars)	Cavity Radius (meters)	Cavity Pressure (bars)	RDP 3 (m)
Rainier Mesa						
Dido Queen 1	184	117	75	36.34	79.2	5000
Dido Queen 2	189	127	60	36.72	76.3	5700
Mighty Epic	588	319	75	26.54	207.7	950
Yucca Flat Dry Tuff						
1 (weak)	304	174	60	31.70	136.7	2500
2 (strong)	565	310	60	27.57	225.0	1400
Baneberry						
1 (strong)	132	76	60	40.45	53.1	5200
2 (weak)	77	46	60	44.34	38.5	8400

calculation uses a failure surface determined for Diagonal Line alluvium, recognized as a very strong, atypical alluvium, the "weak" calculation is probably a more believable estimate of the residual stresses around the Baneberry cavity.

The residual stresses must prevent the cavity pressure from hydrofracturing the surrounding rock. Table 5 shows cavity pressures obtained from the SKIPPER calculations. These cavity pressures are the least reliable part of the calculations since they are obtained using a simple bubble model described in Section 2 to initiate the explosion. Cavity radius is presented for each calculation at the same yield. Again, the most significant influence on cavity size is the failure envelope, higher strength giving smaller cavities and vice versa. There is a general trend of smaller cavities indicating higher cavity pressures.

A primitive measure of the teleseismic coupling implied by these calculations is given by the steady state value of the reduced displacement potential (RDP) shown for yields corresponding to Baneberry. Data compiled by Savino^[18] of S^3 show that both for regional and teleseismic measurements, Baneberry has the same body wave magnitude as Yucca Flat shots of 4 to 5 times the Baneberry yield. Also, for the same depth of burial, Baneberry has 4 or 5 times the surface wave amplitude. The data based on Bache, et al.^[19] therefore indicates that the average Yucca Flat calculation has the proper RDP relative to the best guess "weak" Baneberry calculation. (RDP varies linearly with yield.) Data from Savino also shows body wave magnitudes from Baneberry comparable to typical Rainier Mesa events. This tends to indicate that either Baneberry calculation would be satisfactory, with the "strong" being slightly preferred.

Other Baneberry calculations were made; one varying the magnitude of the yield strength in layer 1 (the high clay

content WP layer), and another the location of the interface between layers 1 and 2. These calculations showed that the strength and location of layer 1 had no influence on the peak residual stress which occurred in layer 2 for all calculations. The strength and location of layer 1 did influence cavity size and therefore cavity pressure.

Figures 2-7 show the complete residual stress fields for the calculations of Table 5 (Dido Queen 1 is not included since it is almost identical to Dido Queen 2). Note that the overburden pressure has not been subtracted out from these stresses. It is observed that higher strength not only increases the peak residual stress, it also makes the peak values occur closer to the WP. (This is partially a consequence of smaller cavity size.) For lower strengths, the stress field is spread out over a considerably greater volume, however. All the calculations considered the medium to be infinite in extent and, so, neglected free surface effect. However, the free surface will have the effect of reducing the magnitude of these residual stresses. For Baneberry, where the free surface is only 278 meters from the working point, well within the calculated residual stress field, the residual stress field would be greatly affected. Although these results cannot be considered definitive evidence, they are instructive and thought provoking. They strongly suggest that devices should be buried more deeply in a weaker medium.

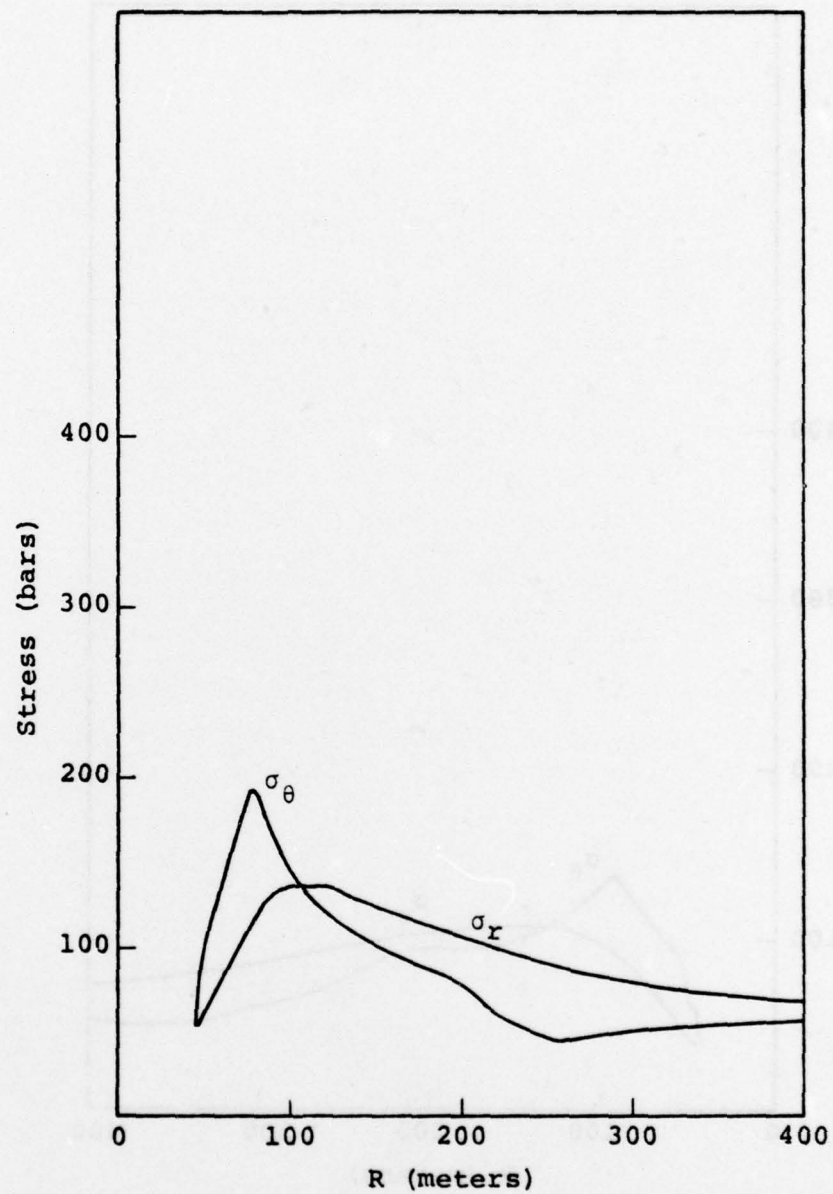


Figure 2. Residual stress field versus position for Baneberry 1 (strong).

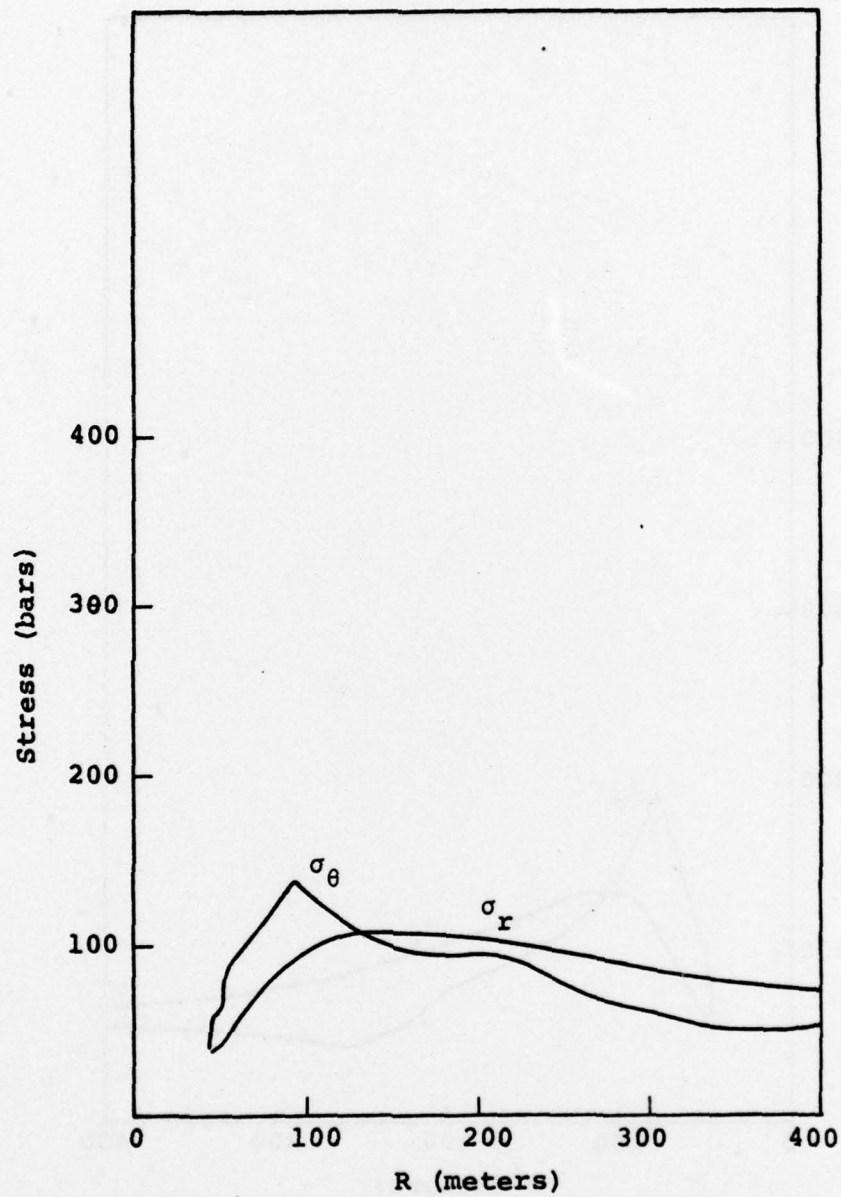


Figure 3. Residual stress field versus position for Baneberry 2 (weak).

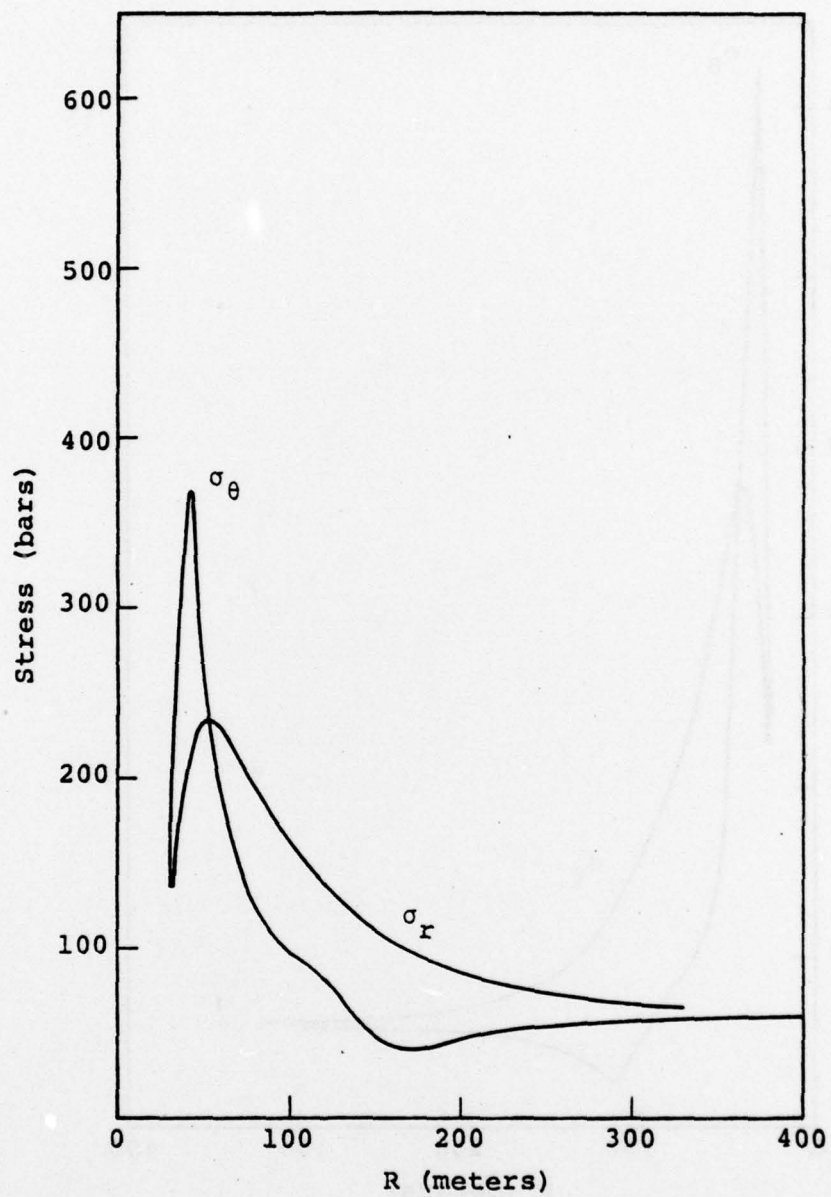


Figure 4. Residual stress field versus position for Yucca Flat 1 (weak).

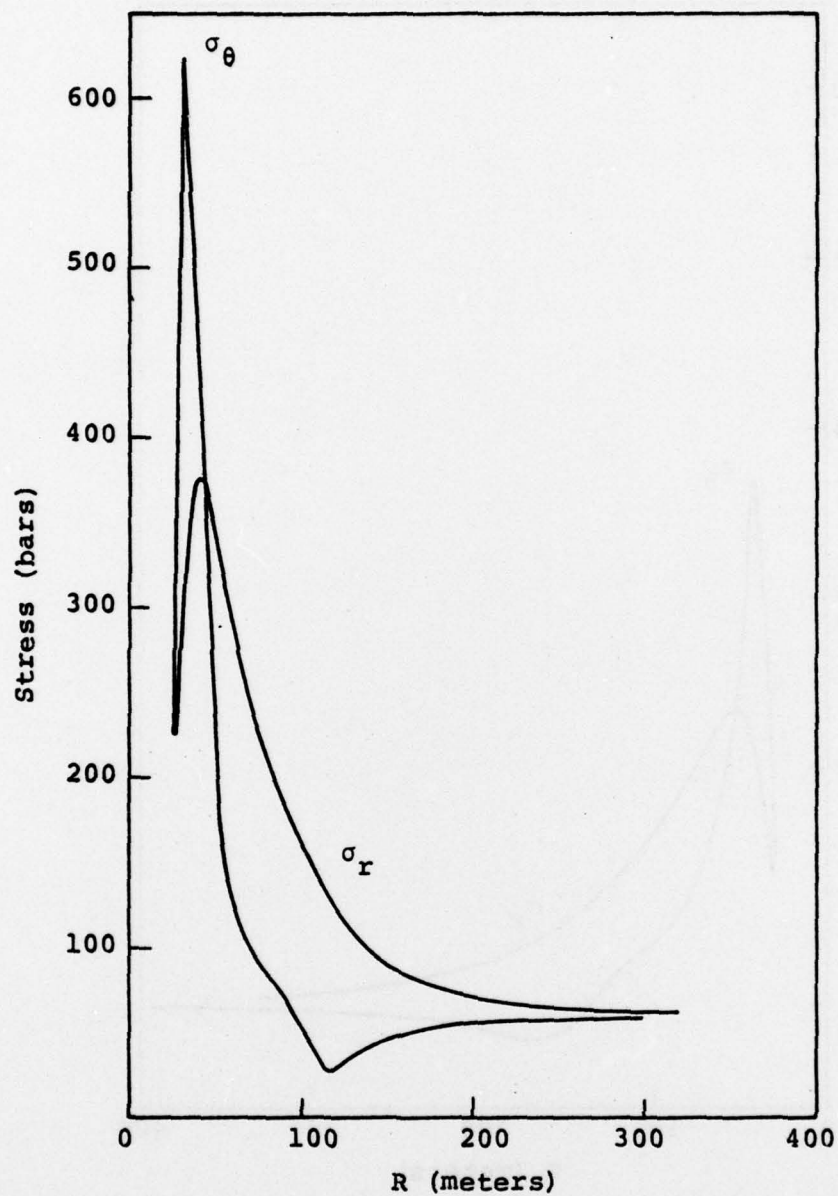


Figure 5. Residual stress field versus position for Yucca Flat 2 (strong).

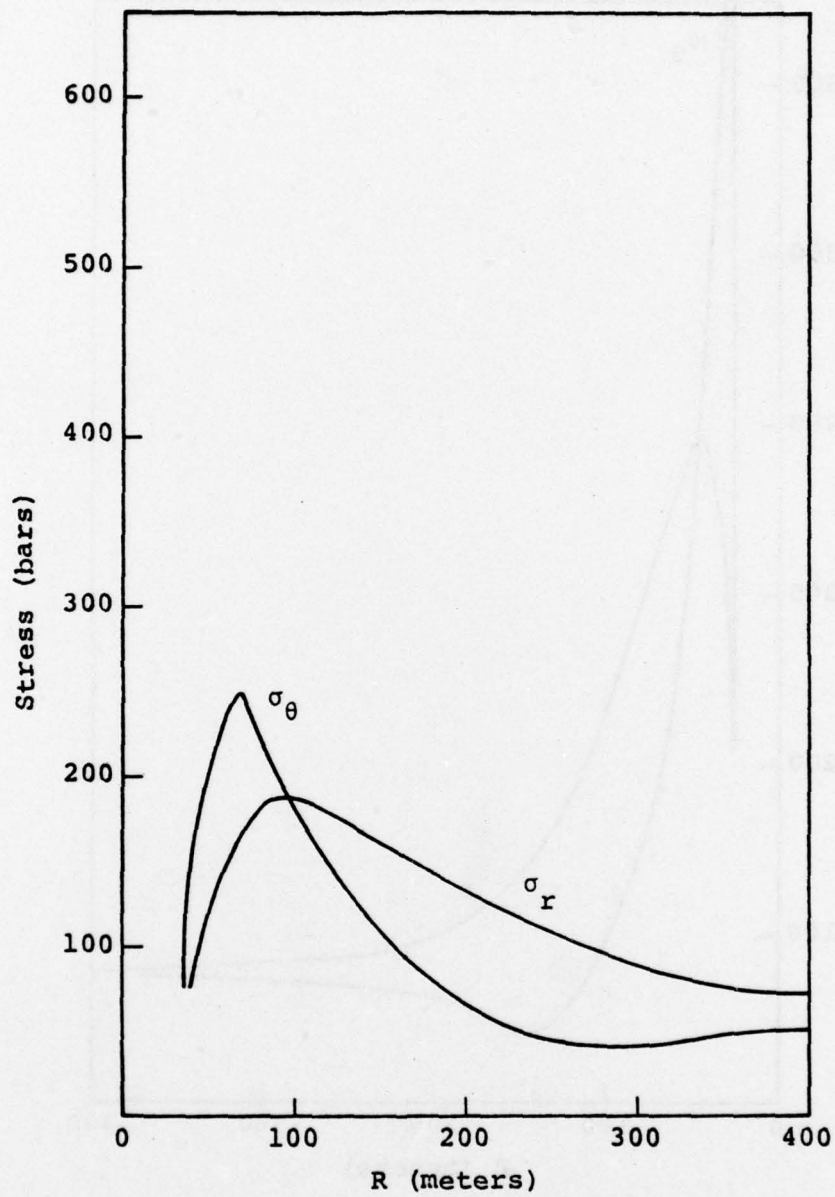


Figure 6. Residual stress field versus position for Dido Queen.

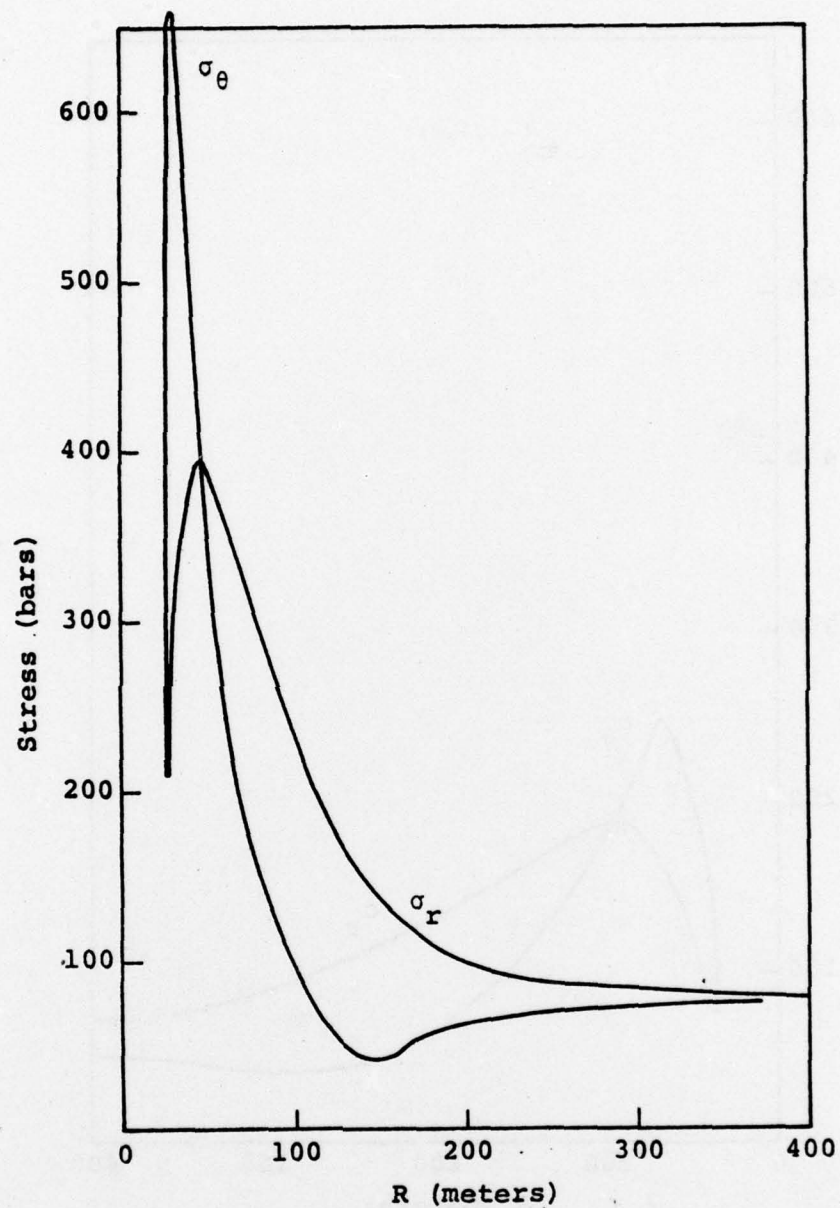


Figure 7. Residual stress field versus position for Mighty Epic.

5. FIGURES OF MERIT

It is difficult to quantify what is important to containment of the cavity gases when comparing the calculations of Table 5 (Section 4). Some possible "figures of merit" are discussed in this section. In Reference 4, and in Section 4 of this report, the values of the peak residual stresses (particularly the hoop stresses), relative to the scalar overburden pressure, were compared. It is reasonable to use the stresses with the overburden subtracted out as a measure of containment since the philosophy is that it is the additional stresses over the overburden which forms the containment membrane to prevent hydrofracture from the cavity. There it was stated that containment was better when the peak residual stresses were higher.

This simple figure of merit does not give the complete picture, however. Figures 2-7 show that the residual stress fields look quite different for strong media (where the peak stresses are high) and weak media. For weak media, the compressive hoop stresses, though smaller in magnitude, tend to occur over a larger radial distance, i.e., the residual stress membrane is thicker. However, we believe that a thinner, but significantly higher stress membrane is far more effective as a containment membrane, so that we will continue to use the peak residual stress in our figure of merit.

Of course, these residual stresses must resist a cavity pressure. Based on the simple mechanics of materials problem of a thin walled pressure vessel, the ratio of cavity pressure to peak transverse residual stress would appear to be a reasonable figure of merit. However, the cavity pressure computed using SKIPPER is not a good measure of the real cavity pressure. It takes no account of water getting into the cavity from the surrounding rock or of additional thermal equilibration expected in the rock outside the calculated

cavity. A procedure developed by Peterson and Lie^[20] to obtain cavity pressures and temperatures for cavity leak calculations was modified here and used to calculate a better value of cavity pressure from the output of the SKIPPER calculations.

Starting from the final state obtained from the SKIPPER output (cavity radius, cavity energy, internal energy and mass of adjacent zones, etc.) and beginning at the cavity boundary, small amounts of mass of rock (and its accompanying internal energy) are equilibrated with the melted cavity material which is at a specific internal energy greater than the melt energy of the rock. This calculational procedure approximates the physical processes of spall and equilibration. The process is stopped when sufficient mass has been added so that the equilibrated "cavity" is at the melt energy. Finally, the volume of steam in the new cavity is computed based on the water content of the undisturbed rock, and a final cavity pressure is calculated (for the steam).

One question which arises involves how much water is in the undisturbed rock. The water content by weight, f_w , given in Table 2 of Section 2, is defined as the amount of water that can be removed at 105°C. This does not include the bound water in the rock. For Rainier Mesa tuff, this amounts to approximately 7 percent extra water by weight.^[20] The cavity pressure was computed for each of the calculations shown in Table 5, using f_w alone and also including the additional bound water (assumed to be 7 percent for all media). Table 6 presents the results of these computations. Note that the effect of equilibrating the cavity with the outside material is to reduce the cavity pressure for all cases. When the bound water is included in the computation of cavity pressure, less of a change results, as would be expected. (The mass of rock material reduces the pressure while the water tends to increase it.)

Table 6
Figures of Merit for Equilibrated and Unequilibrated Cavities

Event	f_w	Peak Transverse Residual Stress σ_t (bars)	Equili- brated Cavity Radius (meters)	Unequili- brated Cavity Pressure, P_1 (bars)	Equilibrated Cavity Pressure (bars)			Figures of Merit		
					No Bound Water P_2	Bound Water P_3		$\frac{P_1}{\sigma_t}$	$\frac{P_2}{\sigma_t}$	$\frac{P_3}{\sigma_t}$
Rainier Mesa										
Dido Queen 1	0.16	184	36.70	79.3	39.4	55.4		0.43	0.21	0.30
Dido Queen 2	0.16	189	37.09	76.3	36.5	54.9		0.40	0.19	0.29
Mighty Epic	0.17	588	27.40	207.7	101.4	147.6		0.35	0.17	0.25
Yucca Flat Dry Tuff										
1 (weak)	0.13	304	32.18	136.7	51.8	84.1		0.45	0.17	0.27
2 (strong)	0.13	565	28.35	225.0	95.4	152.2		0.40	0.17	0.27
Baneberry										
1 (strong)	0.22	132	40.62	53.1	34.6	47.1		0.40	0.26	0.36
2 (weak)	0.22	77	44.49	38.5	24.0	32.4		0.50	0.31	0.42

Here, σ_t is the peak transverse residual stress and the figures of merit chosen are ratios of the calculated cavity pressures, P_1 , P_2 and P_3 to σ_t . Let us define a higher ratio of cavity pressure to σ_t as a greater relative containment risk. For both the figures of merit in which cavity pressure from an equilibrated cavity was used, both Baneberry calculations are clearly less conservative and therefore relatively greater containment risks. Using the unequilibrated cavity pressure, the "weak", best guess, Baneberry 2 calculation is the worst risk. However, the "strong" Baneberry 1 calculation lies within the data for the other events.

Summarizing, for all figures of merit investigated, the "best guess" Baneberry 2 calculation is clearly the worst risk. Only when the unequilibrated cavity pressure (a hardly justifiable choice) is used, does even the strong upper limit Baneberry 1 calculation appear as safe as for other events.

REFERENCES

1. U. S. Geological Survey Report, "Results of Exploration of Baneberry Site, Early 1971," USGS-474-145, July 1974.
2. Ramspott, L. D., private communication, Lawrence Livermore Laboratory, 1975.
3. Butters, S. W., Terra Tek, letter to Mr. Carl Keller, DNA Field Command, May 25, 1976.
4. Rimer, N., "A Scenario for the Containment Failure of Baneberry," Systems, Science and Software Topical Report SSS-R-75-2703, August 1975.
5. Rimer, N., "The Relationship Between Material Properties, Residual Stresses, and Cavity Radius Due to a Nuclear Explosion," Systems, Science and Software Topical Report SSS-R-76-2907, May 1976.
6. Cherry, J. T., N. Rimer and W. O. Wray, "Seismic Coupling from a Nuclear Explosion: The Dependence of the Reduced Displacement Potential on the Nonlinear Behavior of the Near Source Rock Environment," Systems, Science and Software Report SSS-R-76-2742, September 1975.
7. Tillotson, J. H., "Metallic Equations of State for Hypervelocity Impact," General Atomic Report GA-3216, July 1962.
8. Cherry, J. T. and F. I. Peterson, "Numerical Simulation of Stress Wave Propagation from Underground Nuclear Explosions," Engineering with Nuclear Explosives, ANS, USAEC, Conf. 700101, 1970.
9. Maenchen, G. and S. Sack, "The TENSOR Code," in Methods in Computational Physics, Vol. 3, Academic Press, New York, 1964.
10. Laird, D. H., "A Chemical Equilibrium Equation of State for Saturated Tuff," Systems, Science and Software Topical Report SSS-R-75-2740, January 1976.
11. Stephens, D. R., H. C. Heard and R. N. Schock, "Preliminary Equation of State Data for Baneberry Altered Tuff," Lawrence Livermore Laboratory Memorandum UCID-15874, July 13, 1971.

12. Butters, S. W., R. J. Reid, S. J. Green and A. H. Jones, "Mechanical Properties of Nevada Test Site Tuff from Selected Exploratory Drill Holes," Terra Tek, Inc. Final Report TR 73-28, July 1973.
13. Rimer, N., R. Herrmann and R. Duff, "A Calculation of the Interface Motion from the Mighty Epic Event," Systems, Science and Software Topical Report SSS-CR-77-3056, November 1976.
14. Ramspott, L. D. and N. W. Howard, "Average Properties of Nuclear Test Areas and Media at the USERDA Nevada Test Site," Lawrence Livermore Laboratory Report UCRL-51948, September 15, 1975.
15. App, F. N., Los Alamos Scientific Laboratory, letter to Dr. Russell Duff, Systems, Science and Software, June 7, 1976.
16. Heard, H. C. and D. R. Stephens, "Compressibility and Strength Behavior for Diagonal Line Alluvium," Lawrence Radiation Laboratory Report UCID-15736, October 14, 1970.
17. Bonner, B. P., A. E. Abey, H. C. Heard and R. N. Schock, "High-Pressure Mechanical Properties of Merlin Alluvium," Lawrence Livermore Laboratory Report UCRL-51252, July 7, 1972.
18. Savino, J., private communication, April 1977.
19. Bache, T. C., T. G. Barker, N. Rimer, T. R. Blake, D. G. Lambert, J. T. Cherry and J. M. Savino, "An Explanation of the Relative Amplitudes of the Teleseismic Body Waves Generated by Explosions in Different Test Areas at NTS," Systems, Science and Software Final Report DNA 3958F, October 1975.
20. Peterson, E. W. and K. Lie, "Hudson Moon Leak Evaluation," Systems, Science and Software Topical Report (in preparation).

DISTRIBUTION LIST

DEPARTMENT OF DEFENSE

Defense Documentation Center
Cameron Station
12 cy ATTN: TC

Director
Defense Nuclear Agency
ATTN: DDST
ATTN: TISI
3 cy ATTN: TITL

Commander
Field Command
Defense Nuclear Agency
ATTN: FCPR
ATTN: FCTMC, Carl Keller

Director of Defense Research & Engineering
Department of Defense
ATTN: S&SS (OS)

Chief
Livermore Division, Field Command, DNA
Lawrence Livermore Laboratory
ATTN: FCPRL

Chief
Test Construction Division
Field Command Test Directorate
Defense Nuclear Agency
ATTN: NTS, Joe LaComb

DEPARTMENT OF THE ARMY

Commander
Harry Diamond Laboratories
ATTN: DRXDO-NP

DEPARTMENT OF THE NAVY

Officer-in-Charge
Naval Surface Weapons Center
ATTN: Code WA501, Navy Nuc. Prgms. Off.

DEPARTMENT OF THE AIR FORCE

AF Weapons Laboratory
ATTN: SUL

ENERGY RESEARCH & DEVELOPMENT ADMINISTRATION

University of California
Lawrence Livermore Laboratory
ATTN: David Oakley
ATTN: Billy Hudson
ATTN: Mr. Terhune

ENERGY RESEARCH & DEVELOPMENT ADMINISTRATION (Continued)

Los Alamos Scientific Laboratory
ATTN: Robert Brownlee
ATTN: Fred App

Sandia Laboratories
ATTN: Wendell Weart/Lynn Tyler

US Energy Research & Development Admin.
Nevada Operations Office
ATTN: Robert Newman

OTHER GOVERNMENT AGENCY

Department of Commerce
US Geological Survey
Special Projects Branch
ATTN: Rod Carroll

DEPARTMENT OF DEFENSE CONTRACTORS

Pacifica Technology
ATTN: G. I. Kent

Physics International Company
ATTN: E. T. Moore

SRI International
ATTN: Alex Florence

Systems, Science & Software, Incorporated
ATTN: Russell E. Duff
ATTN: Norton Rimer

Terra Tek, Incorporated
ATTN: Sidney Green

General Electric Company
TEMPO-Center for Advanced Studies
ATTN: DASIAC

AD-A049 220

SYSTEMS SCIENCE AND SOFTWARE LA JOLLA CALIF

F/G 18/3

THE INFLUENCE OF CLAY AND WATER IN ROCKS ON CONTAINMENT OF UNDE--ETC(U)

JUN 77 N RIMER

DNA001-77-C-0099

UNCLASSIFIED

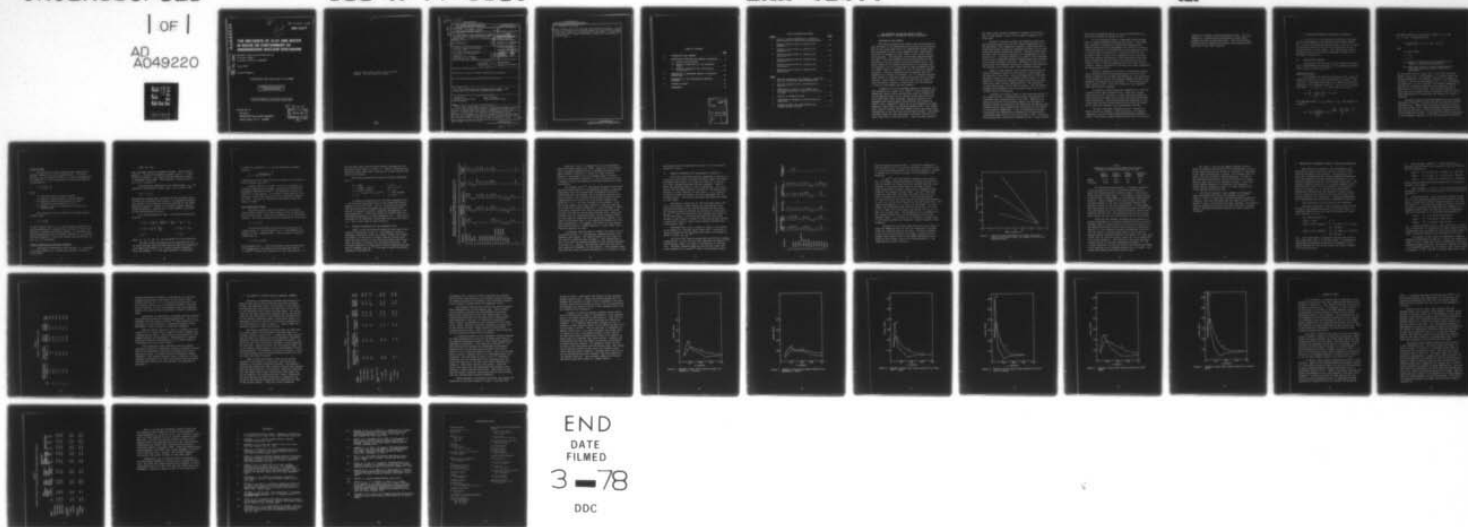
SSS-R-77-3339

DNA-4347T

MI

| OF |

AD
A049220



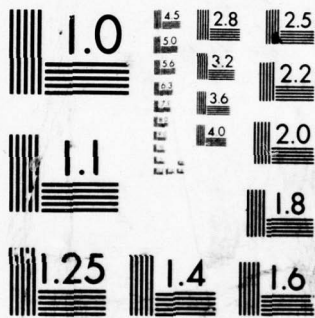
END

DATE

FILMED

3-78

DDC



MICROCOPY RESOLUTION TEST CHART
NATIONAL BUREAU OF STANDARDS-1963-A

AD A 049220

DDC FILE COPY

AD-E 300 034

DNA 4347T

THE INFLUENCE OF CLAY AND WATER IN ROCKS ON CONTAINMENT OF UNDERGROUND NUCLEAR EXPLOSIONS

Systems, Science and Software
P.O. Box 1620
La Jolla, California 92038

June 1977

Topical Report

CONTRACT NO. DNA 001-77-C-0099

APPROVED FOR PUBLIC RELEASE;
DISTRIBUTION UNLIMITED.

THIS WORK SPONSORED BY THE DEFENSE NUCLEAR AGENCY
UNDER RDT&E RMSS CODE B345077462 J24AAXYX98349 H2590D.

Prepared for
Director
DEFENSE NUCLEAR AGENCY
Washington, D. C. 20305

DDC
RECEIVED
JAN 27 1978
RECEIVED
A

Destroy this report when it is no longer
needed. Do not return to sender.



SECURITY CLASSIFICATION OF THIS PAGE (When Data Entered)

DD FORM 1 JAN 73 1473

SECURITY CLASSIFICATION OF THIS PAGE (When Data Entered)

388 507

UNCLASSIFIED

SECURITY CLASSIFICATION OF THIS PAGE(When Data Entered)

20. ABSTRACT (Continued)

shear strength due to the abnormal clay and water contents. Calculations with these lower strengths showed far lower residual stress fields when compared to calculations for other media. A discussion of the relevance of these calculational results to containment is presented. ←

UNCLASSIFIED

SECURITY CLASSIFICATION OF THIS PAGE(When Data Entered)

TABLE OF CONTENTS

	<u>Page</u>
1. INTRODUCTION AND SUMMARY.	3
2. CONSTITUTIVE MODELING AND MATERIAL PROPERTIES . .	7
2.1 Constitutive Modeling.	7
2.2 Material Properties for the Parameter Study.	12
2.3 Material Properties for Calculations of Section 4	15
3. SENSITIVITY OF BANEERRY RESULTS TO MODELING ASSUMPTIONS	21
4. THE EFFECT OF CLAY AND WATER ON RESIDUAL STRESSES.	25
5. FIGURES OF MERIT.	35
REFERENCES.	39

ACCESSION FOR	
NTIS	White Section <input checked="" type="checkbox"/>
DOC	Buff Section <input type="checkbox"/>
UNANNOUNCED	<input type="checkbox"/>
JUSTIFICATION	
BY	
DISTRIBUTION/AVAILABILITY CODES	
Dist.	AVAIL. and/or SPECIAL
A	

LIST OF FIGURES AND TABLES

<u>Figure</u>		<u>Page</u>
1	Uniaxial stress difference at 4 kbars vs. water content for Terra Tek laboratory data. . . .	18
2	Residual stress field vs. position for Baneberry 1.	29
3	Residual stress field vs. position for Baneberry 2.	30
4	Residual stress field vs. position for Yucca Flat 1	31
5	Residual stress field vs. position for Yucca Flat 2	32
6	Residual stress field vs. position for Dido Queen	33
7	Residual stress field vs. position for Mighty Epic.	34

<u>Table</u>		
1	Material properties for Baneberry, Yucca Flat dry tuff and Rainier Mesa saturated tuff	13
2	Material properties for calculations of Section 4.	16
3	Comparison of results using TAMEOS and Tillotson equations of state for Yucca Flat dry tuff	19
4	Results of parameter study	23
5	Comparison of Baneberry, Rainier Mesa and Yucca Flat	26
6	Figures of merit for equilibrated and unequilibrated cavities.	37

THE INFLUENCE OF CLAY AND WATER IN ROCKS ON CONTAINMENT OF UNDERGROUND NUCLEAR EXPLOSIONS

1. INTRODUCTION AND SUMMARY

This report discusses the effects that large amounts of clay and water in the surrounding rock may have on the containment of hot cavity gases due to an underground nuclear event. The containment failure of the Baneberry event, detonated in Yucca Flat in December of 1970, seems to be an ideal vehicle for this study. The Baneberry site has been characterized by the USGS^[1] as having unusually high concentrations of montmorillonite clay (65 percent) around the working point. The water content of the working point material (an altered tuff) is related to the clay content and has been estimated by both the USGS^[1] and by L. Ramspott^[2] to be as much as 25 percent by weight. Material properties data for Rainier Mesa tuff, compiled by S. Butters of TerraTek, Inc.^[3] indicate that high water content in laboratory samples correlates with low shear strength. While there is little hard data on the effect of clay on material strength, it seems clear that the presence of clay can only weaken the host material.

A scenario for the containment failure of Baneberry has been presented in a report by N. Rimer^[4] which discusses one-dimensional ground motion calculations using the SKIPPER code of the Baneberry event and of typical Rainier Mesa and Yucca Flat events which were contained. Material properties for Baneberry were based on site investigations and analyses by USGS^[1] and L. Ramspott^[2] which led to the assumption of three spherical layers about the Baneberry working point. The working point layer of altered tuff was assumed to have negligible shear strength due to the very high clay and water content. The second and third layers for the calculations were both alluvium (the third layer was of infinite extent). Since the clay content of

the second layer had been estimated at between 20 and 50 percent, it was assumed to have half the shear strength of the third layer.

The major difference between the Baneberry calculation and the Rainier Mesa and Yucca Flat results appeared to be in the magnitude of the compressive residual stress fields due to nonuniform plastic loading and subsequent unloading of the rock around the explosion-produced cavities. Residual stress fields are seen after the cavity rebounds in all ground motion calculations at S^3 . Parameter studies by N. Rimer^[5] have indicated that the peak transverse residual stresses depend very strongly on the shear strength of the rock. Therefore, it was not surprising that the Baneberry calculation, modeled with relatively low strength, gave significantly lower residual stresses.

Based on these results, the following scenario was presented as possibly leading to the venting of cavity gases to the surface at late times. The low strength due to high clay and water content led to low residual stress fields. In the absence of a significant residual stress field, the hot cavity gases could cause tensile hydrofracturing. The fracturing, if sufficiently great, could lead to venting. The low material strength was considered to be the primary reason for the containment failure of Baneberry.

Although the original report of this work was written in the summer of 1975, it received only limited distribution to interested ERDA representatives at the time. Because of the general sensitivity of the subject matter, we were asked to withhold further distribution until additional calculations were completed which would determine the sensitivity of the results to the modeling assumptions. A set of suggested multi-layer calculations was completed and presented at an Earth Motion Calculators meeting held in La Jolla on May 4, 1976. Since the multi-dimensional calculations requested in Ref. 4 have recently

been done and presented by LLL at the 66th CEP meeting, the report was released in January of 1977.

In the intervening period, considerable work has been done to clarify questions raised by that report. The present work includes a discussion of constitutive modeling and material properties data improvements (see Section 2) used in later calculations of both Baneberry and the comparison events in Rainier Mesa and Yucca Flat. It was felt that the comparisons in Ref. 4 might not be completely valid since there were some modeling differences in the calculations being compared (the Rainier Mesa and Yucca Flat calculations, as described in Ref. 4, were not made specifically as part of this program.) Careful consideration has shown that those comparisons are qualitatively valid.

Section 3 describes the results of calculations presented at the Earth Motion Calculators meeting of May 4, 1976. Based on suggestions from ERDA representatives, the sensitivity of the results to some of the modeling assumptions used in the Baneberry calculation was investigated. It was found that the basic results of Ref. 4 were not sensitive to any parameter other than material strength.

In Section 4, calculations are presented for a weak and a strong Rainier Mesa saturated tuff, a weak and a strong Yucca Flat dry tuff, as well as a weak, best-guess Baneberry calculation and an upper-limit, relatively-high-strength Baneberry calculation. These calculations show Baneberry to have a much lower residual stress field than the other NTS events due to the lower strength of the surrounding alluvium.

Section 5 discusses "figures of merit," measures by which one can tell whether a particular event is a greater containment risk than other previously-detonated successful events. The figure of merit chosen was the ratio of the cavity

pressure to the peak transverse residual stress. For this comparison, a sophisticated determination of the cavity pressure was used as described below. Using the resulting figure of merit, Baneberry was clearly the greatest containment risk of the events examined.

2. CONSTITUTIVE MODELING AND MATERIAL PROPERTIES

In Section 2.1, the constitutive models are discussed briefly with emphasis on the modeling improvements between Ref. 4 and the calculations presented here. Section 2.2 gives the material properties used for the calculations of Ref. 4 and of Section 3 of this report. The modeling and material properties used for the results presented in Section 4 are discussed in Section 2.3.

2.1 CONSTITUTIVE MODELING

Descriptions are given here of the constitutive models used in the SKIPPER calculations. A more complete discussion may be found in Cherry, et. al.^[6]

Equations of State

The Baneberry calculations described in Ref. 4 used an equation of state of the form developed by Tillotson^[7] and fit at S^3 to available shock data for a number of geological materials. For compressed states ($\rho > \rho_0$) and for cold expanded states ($\rho < \rho_0$ and $e < e_s$), the pressure is given by

$$P_s = \left[a + \frac{b}{\frac{e}{e_0 \eta^2} + 1} \right] e \rho + A \mu + B \mu^2 \quad .$$

For expanded states ($\rho < \rho_0$) where $e > e_s$, the pressure is given by

$$P_v = a e \rho + \left[\frac{b e \rho}{\frac{e}{e_0 \eta^2} + 1} + A \mu e^{-\beta \left(\frac{\rho_0}{\rho} - 1 \right)} \right] e^{-\bar{\alpha} \left(\frac{\rho_0}{\rho} - 1 \right)^2} \quad .$$

The phase transition from liquid to vapor ($\rho < \rho_0$ and $e_s < e < e'_s$) is approximated as

$$P = \frac{1}{e'_s - e_s} \left[(e - e_s) P_v + (e'_s - e) P_s \right] .$$

Here

ρ = mass density

$\eta = \rho/\rho_0$

$\mu = \eta + 1$

e_s = specific internal energy as the material is brought to vaporization temperature

e'_s = additional specific internal energy required to change the material from a liquid to a vapor state

All the above formulas assume that no air-filled voids are present in the rock. The constants, a , b , and e_0 govern the energy dependence of the material, allowing it to behave as an ideal, γ -law gas at high energies ($a \sim \gamma - 1$), and reducing the effective γ at lower energies. The density dependence is governed by a quadratic polynomial with constants A and B which may be fit to shock data. The Tillotson equation of state does not accurately model the expansion from rock states above approximately 10 kbars where the expansion of steam is important.

The Tabular Array of Mixtures Equation of State (TAMEOS) described in Cherry^[6] has been used for all tuff calculations discussed here. TAMEOS mixes the proper percentage of water with grain density rock, assuming pressure equilibrium between the rock and the water, to give the pressure response for the fully crushed tuff mixture. This gives a far better description of the subsequent expansion of the shocked water-rock mixture.

Porous Crushup

The equations of state discussed above describe the pressure response for fully saturated rocks. Air-filled porosity ϕ_0 is included through the S^3 porous crushup model (P- α model) [6] in which the pressure of the porous material is described by

$$P = \frac{1}{\alpha} \bar{P} \left(\frac{V}{\bar{V}}, e \right)$$

where

V = specific volume of porous material

e = specific internal energy of porous material

\bar{P} = pressure obtained from equation of state

α = distension ratio defined by $V/\bar{V} \geq 1$

\bar{V} = specific value of the material with zero air-filled voids

The distension ratio is required to decrease from an initial value

$$\alpha_0 = \frac{1}{1 - \phi_0}$$

at zero pressure down to 1.0 as the pressure increases to P_c , the crush pressure or pressure limit at which all air-filled porosity is assumed irreversibly removed. Any porosity lost during compression below the elastic pressure P_e is recoverable upon expansion. Any porous crushup occurring between P_e and P_c is irreversible.

Elastic Properties and Material Strength

The ambient compressional wave velocity C_0 is related to the bulk modulus K_0 and the shear modulus G by the relationship

$$\rho_0 C_0^2 = K_0 + \frac{4}{3} G$$

Here, the shear modulus is assumed constant. Since the bulk modulus K varies with pressure, Poisson's ratio σ is not being held constant. One calculation was made with constant σ throughout the crushup. This requires a constant ratio of K/G , i.e., a varying G .

The deviatoric components of the stress tensor S_{ij} are related to the deviatoric strain rates $\dot{\epsilon}_{ij}$ by Hooke's law

$$\dot{S}_{ij} = 2 G \dot{\epsilon}_{ij}$$

The material strength model requires that the principal stress be within the von Mises yield surface. For spherical geometry, this reduces to the condition that the magnitude of the radial deviatoric stress not exceed 2/3 the yield strength (maximum stress difference). Behavior of a failed element is governed by the non-associated flow rule.

For the calculations of Ref. 4, the yield strength was given by

$$Y = \left[Y_0 + Y_m \frac{P}{P_m} \left(2 - \frac{P}{P_m} \right) \right] \left(1 - \frac{e}{e_m} \right) \quad P < P_m, e < e_m$$

$$Y = \left(Y_0 + Y_m \right) \left(1 - \frac{e}{e_m} \right) \quad P \geq P_m, e < e_m$$

$$Y = 0 \quad , \quad e > e_m$$

where Y_0 , Y_m , P_m and e_m are constants for a given material.

The more recent calculations use an improved form for the yield strength which has been shown by Cherry and Peterson^[8] to be empirically superior to a simple pressure dependence. Here, the pressure P in the above equations is replaced by

\bar{P} which is a function of P and the deviatoric stresses given by

$$\bar{P} = P - \frac{1}{2} \left(\frac{S_{11}S_{22}S_{33}}{2} \right)^{1/3}$$

A description of how shear failure is treated in this model is given in Cherry, et. al. [6]

Tension failure is allowed to occur in an element if a principal stress becomes tensile. The tension failure model proposed by Maenchen and Sack [9] and described in detail by Cherry [6] is then applied. An inelastic strain which is just sufficient to zero the tensile stress is introduced normal to the crack. This strain increases or decreases as the crack opens or closes.

Cavity Equation of State

The cavity source region was chosen to be initially large enough to vaporize 70 metric tons of rock for each kiloton of device yield. (The rock is assumed to be at undisturbed density.) The cavity pressure for all calculations is given by

$$P = (\gamma - 1) e/V$$

For the Rainier Mesa and Yucca Flat calculations described in Ref. 4, γ was set equal to 1.5. The Baneberry calculation of Ref. 4 assumed that γ was a function of specific volume given by

$$\gamma = 1.03 + 0.9/\sqrt{V}$$

This expression for γ was a preliminary result obtained for tuff modeled using the chemical equilibrium CHEST code of D. Laird [10] and has been modified for later calculations. It

will be shown later that the peak residual stresses are not sensitive to the choice of cavity γ . However, depending upon the cavity model used, peak velocities at a given location may differ by 20 percent.

More recent calculations used the following expression for γ .

$$\begin{array}{ll} \gamma' = 1.085 & V \geq 1.9 \\ \gamma' = 1.2085 - 0.065 V & 1.9 > V \geq 0.9 \\ \gamma' = 1.9375 - 0.875 V & V < 0.9 \\ \gamma = \gamma' - 0.032 + 3.2 \times 10^{-13} e & e > 10^{11} \text{ ergs/gm} \\ \gamma = \gamma' & e \leq 10^{11} \end{array}$$

It should be emphasized that the above expressions for γ are only very approximate fits to the complicated tabular equation of state of Laird. The fit given above was derived from data from a table developed for one particular water content (24 percent by weight, including approximately 7 percent bound water). Since the creation of a CHEST table is a complicated procedure, the same expression for γ was used in calculations for Baneberry, Rainier Mesa and Yucca Flat tuffs, i.e., over a wide range of water contents.

2.2 MATERIAL PROPERTIES FOR THE PARAMETER STUDY

Table 1 gives the material properties data used in the original calculations of Ref. 4. For Baneberry, Material 1 describes a saturated, high clay content altered tuff extending radially 15.24 meters (50 feet) from the working point. Since the clay content of this layer was greater than 50 percent, the material strength was considered negligible. The Tillotson equation of state, using constants approximating the data of Stephens, et. al.,^[11] was used to model the pressure response of the material.

Table 1
Material properties for Baneberry, Yucca Flat dry tuff
and Rainier Mesa saturated tuff (Reproduced from Ref. 4)

Property	Baneberry			Yucca Flat	Rainier Mesa
	Material 1	Material 2	Material 3		
ρ_o (gm/cm ³)	1.91	2.128	2.016	1.7	1.91
c_o (km/sec)	1.607	2.086	1.606	2.13	2.34
G (kbar)	7	30	15	25.8	35.7
k_o (kbar)	40	50	32	55	57.2
ϕ_o	0	0.05	0.10	0.1564	0.012
Y_m (kbar)	0	0.05	0.10	0.62	0.18
Y_o (kbar)	0	0.007	0.007	0.12	0.055
P_m (kbar)	0	0.7	0.7	0.4	0.4
P_e (kbar)	--	0.07	0.07	0.18	0.05
P_c (kbar)	--	2.0	2.0	4.36	1.5
P_o (kbar)	0.060	0.060	0.060	0.096	0.056
e_m (10 ¹⁰ erg/gm)	2.15	2.15	2.15	2.0	2.0
e_s (10 ¹⁰ erg/gm)	3.7	3.7	3.7	--	--
e'_s (10 ¹⁰ erg/gm)	17.5	17.5	17.5	--	--
e_o (10 ¹⁰ erg/gm)	10	10	10	--	--
A (kbar)	40	79.3	79.3	--	--
B (kbar)	352	803	803	--	--
a	0.4	0.4	0.4	--	--
b	0.6	0.6	0.6	--	--
f	--	--	--	0.136	0.17
$\frac{f_w}{\alpha}$	5	5	5	--	--
β	5	5	5	--	--

Materials 2 and 3 are assumed to be alluvium modeled using a Tillotson equation of state. Material 2, with greater than 20 percent montmorillonite, is assumed to have half the shear strength of Material 3, which is a weak alluvium. Material 2 was assumed to be 36.58 meters thick (120 feet) and to be surrounded by Material 3. Free surface effects and a radially varying gravitational field were neglected in these calculations.

The measured data^[1,2] upon which the modeling was based was often conflicting since the Baneberry geology is unusually complicated and since the data were accumulated from holes drilled both pre and postshot and in different locations relative to the WP. The log data indicated that Material 2 had a compressional wave velocity 20 to 30 percent greater than Materials 1 or 3. This was included in the modeling. Also, due to the higher clay content, Material 2 had only half the air-filled void content of Material 3. Also included in Table 1 is material properties data used for calculations for Yucca Flat dry tuff and for Rainier Mesa saturated tuff. These calculations were not made specifically for the Baneberry study but were used for comparison with the Baneberry results. As a result, differences exist in the constitutive modeling for the three calculations. For example, both Yucca Flat and Rainier Mesa calculations use a TAMEOS equation of state rather than a Tillotson equation of state.

A parameter study was made to examine the sensitivity of the results of Ref. 4 to the modeling assumptions used in the Baneberry calculation. The starting point for this study is the material properties data of Table 1. The calculations of Ref. 4 all used the pressure dependent failure surface described in Section 2.1. However, the parameter study used the empirically superior \bar{P} dependent failure surface. The parameter study also used the newer functional dependence of γ on specific volume

and energy which was described in Section 2.1 for the cavity equation of state.

2.3 MATERIAL PROPERTIES FOR CALCULATIONS OF SECTION 4

Using the constitutive modeling described in Section 2.1, a series of calculations was made for Rainier Mesa (Dido Queen and Mighty Epic events), for Yucca Flat dry tuff (a calculation using average properties) and for Baneberry. Table 2 gives the properties used for these calculations. All calculations use the TAMEOS equation of state for the working point material, a cavity equation of state where γ is a function of specific volume and energy, and the \bar{P} dependence for the failure surface. This section discusses the properties chosen for each event.

The material properties for the Dido Queen event, density, grain density, water content and compressional wave velocity were obtained from the CEP document for that event. The failure envelope was modeled using Figure 24 of Butters, et. al.^[12] while the crush curve was obtained from Figure 19 of the same report. Dido Queen was chosen for this study because it was located in tunnel e of the Rainier Mesa complex, a tunnel that triaxial loading tests indicate contains relatively weaker tuffs.

The Mighty Epic event, located in tunnel n, was chosen as an example of a stronger Rainier Mesa tuff. The choice of material properties for the Mighty Epic event is discussed in detail in Rimer, et. al.^[13]

The Yucca Flat material properties were based on average properties for a Yucca Flat dry tuff summarized by Ramspott.^[14] Unfortunately, there is no data on the strength of this material. TerraTek laboratory data for Rainier Mesa tunnel bed tuffs compiled by S. Butters^[3] shows a relationship between

Table 2
Material properties for Calculations of Section 4

Property	Rainier Mesa		Yucca Flat		Baneberry 1		Baneberry 2	
	Dido Queen	Mighty Epic	1	2	Layer 1	Layer 2	Layer 1	Layer 2
f_w	0.16	0.17	0.13	-	0.22	0.10	--	--
ϕ_o	0.016	0.02	0.16	-	0	0.07	--	--
Y_o (kbar)	0.065	0.072	0.1	-	0.03	0.08	0.05	0.05
Y_m (kbar)	0.335	0.628	0.53	-	0.05	0.14	0.09	0.09
P_m (kbar)	3.0	1.0	3.0	1.0	2.0	2.0	--	--
e_m (10^{10} ergs/gm)	2.0	2.0	2.0	-	2.15	2.15	--	--
ρ_o (gm/cm ³)	1.92	1.93	1.7	-	2.00	2.11	--	--
ρ_G (gm/cm ³)	2.383	2.46	2.39	-	2.786	2.64	--	--
C_o (km/sec)	2.48	2.64	1.8	-	1.554	1.8	--	--
G (kbar)	35.8	53	18.8	-	10.7	24.5	--	--
K_o (kbar)	70	64	30	-	34	38	--	--
P_e (kbar)	0.1	0.1	0.1	-	--	0.1	--	--
P_c (kbar)	3.5	4.0	4.0	-	--	4.0	--	--
P_o (kbar)	0.075	0.075	0.060	-	0.060	0.060	--	--
A (kbar)	--	--	--	-	--	52.4	--	--
B (kbar)	--	--	--	-	--	1416	--	--

shear strength and water content. It should be emphasized that the data of Ref. 3 is stress difference in uniaxial strain at 4 kbars confining pressure, not the yield strength. However, it should give a relative indicator of the strength of the materials.

F. App^[15] has drawn several straight lines through a plot of strength (stress difference of 4 kbars) vs water content (by weight) for these data which indicate that the shear strength is inversely proportional to the water content. These lines shown in Figure 1 imply that for Baneberry water contents, the strength is quite small. For the lower water content of Yucca Flat tuff above the water table, the plot gave a strength value of 0.63 kb. The yield strength of 0.63 for Yucca Flat tuff water content was apportioned between Y_o and Y_m in the ratio suggested by the Dido Queen data. This leaves the magnitude of P_m yet to be determined. For this reason, two calculations were made for Yucca Flat, one for a P_m of 3.0 kbar, as in Dido Queen, and another for a P_m of 1.0 kbar, as in Mighty Epic. The parameter P_m is as important to the residual stress field as the magnitude of the failure strength itself. A low value of P_m indicates a steeper slope of the failure surface and therefore a higher strength at low pressures.

A Yucca Flat calculation made with the data of Table 2 using the TAMEOS equation of state was compared to one made using the Tillotson equation of state. Tillotson constants A and B for this calculation were chosen to match the zero pressure bulk modulus used in the TAMEOS calculation and to match its zero energy curve at the crush pressure P_c . The comparisons are given in Table 3.

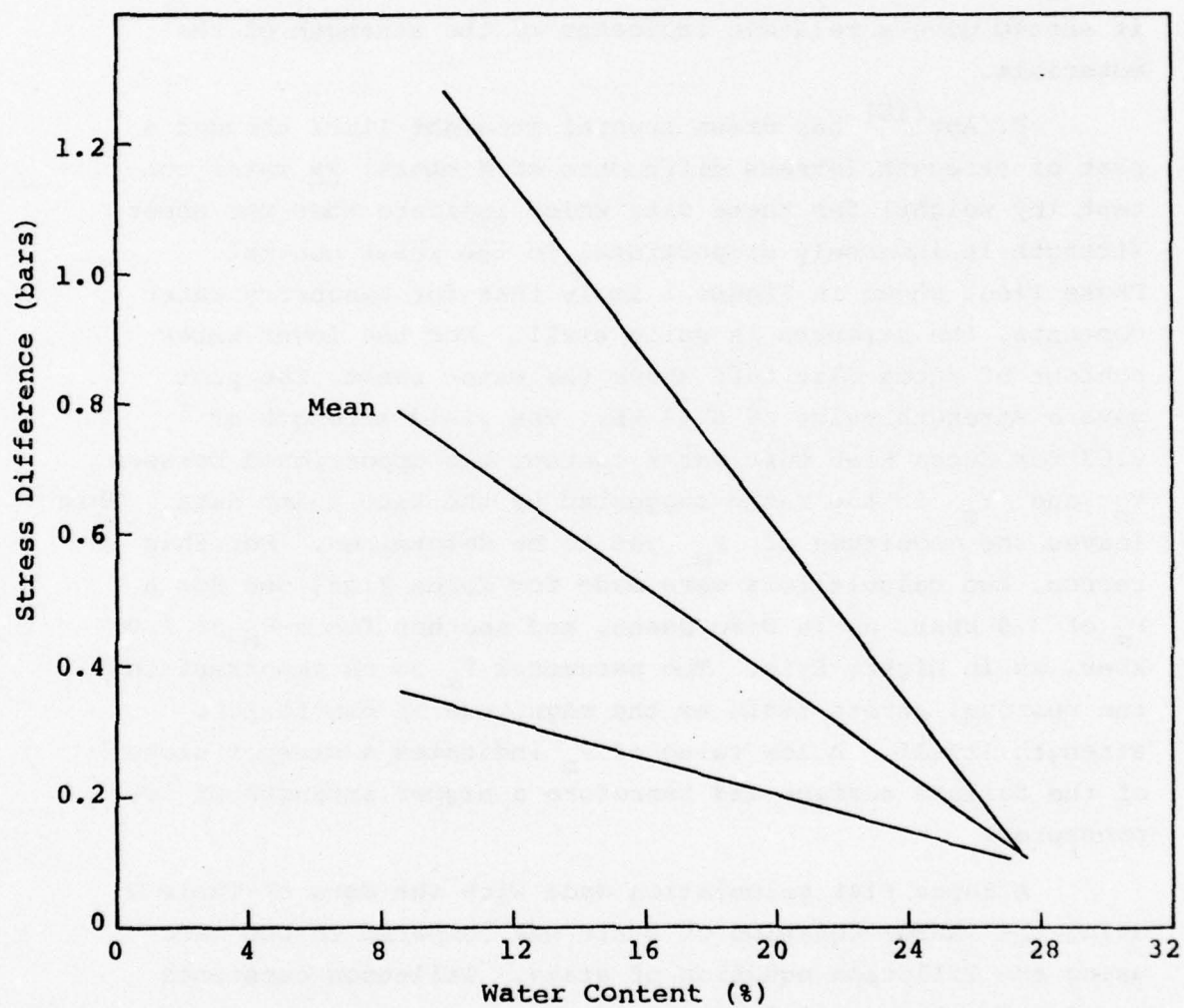


Figure 1. Uniaxial stress difference at 4 kbars (range and mean) versus water content (by weight) for Terra Tek laboratory data.

Table 3
Comparison of results using TAMEOS and Tillotson
equations of state for Yucca Flat dry tuff

	Cavity radius (meters)	Cavity pressure (bars)	Radial stress (bars)	Transverse stress (bars)
TAMEOS	31.70	136.7	174	304
Tillotson	29.18	183.9	140	249

The calculations showed about a 10 percent difference in cavity radius and close to 20 percent differences in radial and transverse peak residual stresses. Cavity pressures were even further apart. On the basis of these results, it was decided to apply TAMEOS to the Baneberry working point material. Input to TAMEOS is the water content (by weight), the grain density of the tuff, and constants defining the equation of state of the grain density tuff. It was assumed that the equation of state constants applicable to Rainier Mesa tuff (having much lower grain densities) may be used for the Baneberry altered tuff. The important features are the high water content and the high grain density due to clay content.

Since the peak residual stresses had been shown to be primarily dependent on the failure strength and not to be very dependent upon the exact position of the layer interface or on the compressional wave velocity (the results are presented in Section 3), it was decided to model the Baneberry site using only two layers, a working point layer of over 50 percent montmorillonite extending radially 35.66 meters (117 feet) from the WP, with an alluvium layer of lower, but still significant clay content around it. The location of the layer was based on data from drill hole Ue8i discussed by Ramspott.^[2] The Tillotson equation of state was used for the second layer which is not expected to see stresses greater than 5-10 kbars. Both layers were modeled using data from hole Ue8i.

For layer 2, data on the failure envelope has been found for Diagonal Line alluvium,^[16] considered to be a relatively strong alluvium and for Merlin alluvium,^[17] considered to be a more representative alluvium. The strength given for layer 2 for the calculation labeled Baneberry 1 in Table 2 was obtained using Diagonal Line alluvium data and so represents an upper limit to the strength of layer 2. The calculation labeled Baneberry 2 is identical with Baneberry 1 except that the strength of layer 2 is lower as shown since it was modeled using Merlin data.

The failure strength of the Baneberry working point layer was modeled using data from Stephens, et. al.^[11] Figure 7 of Ref. 17 plots shear strength vs water contents for alluvium. That plot indicates that for water contents of 20 percent or more, alluvium has zero shear strength. This implies that the working point material may have negligible strength. Figure 1 indicates negligible strength for water contents of 30 percent.

3. SENSITIVITY OF BANEERRY RESULTS TO MODELING ASSUMPTIONS

The results of a parameter study presented at the Earth Motion Calculators meeting held in La Jolla on May 4, 1976 are discussed in this section. The purpose of this study was to answer questions raised by ERDA representatives as to the sensitivity of the results of Reference 4 to the modeling assumptions used for the Baneberry calculation. The material properties used for the 3 material Baneberry base calculation are those used for Reference 4 and are given in Table 1 of Section 2.2. A second look at the modeling assumptions indicated that the thickness of layer 2 (material 2) should be 51.8 meters (170 feet) rather than 36.58 meters (120 feet) as in Reference 4. Modeling improvements were incorporated into this study as described in Section 2.

The calculations of this study are the following:

1. The base calculation: This calculation uses the data of Table 1 but assumes that layer 2 is 170 feet thick. An important feature is that the cavity gas equation of state has a constant γ of 1.5.

The yield strengths are

Layer 1 (clay) $Y = 0$

Layer 2 (half strength) $Y_o = 7.0$ bars, $Y_m = 50$ bars,
 $P_m = 700$ bars

Layer 3 (full strength) $Y_o = 7.0$ bars, $Y_m = 100$ bars,
 $P_m = 700$ bars

- 1a. This calculation is identical with the base calculation except that layer 2 is 120 feet thick. It essentially duplicates the Baneberry calculation of Reference 4 with better modeling for the failure surface and with a constant γ for the cavity gas.

2. High strength, constant γ : This calculation is identical with calculation (1) except for material strengths. The new strengths are

Layer 1 $Y_o = 30$ bars, $Y_m = 10$ bars, $P_m = 700$ bars

Layer 2 $Y_o = 30$ bars, $Y_m = 50$ bars, $P_m = 700$ bars

Layer 3 $Y_o = 30$ bars, $Y_m = 100$ bars, $P_m = 700$ bars

The WP layer has been given some strength and Y_o has been increased in all layers.

3. High strength, $\gamma = g(V,e)$: This calculation duplicates calculation (2) with the cavity equation of state described in Section 2.1.

4. High sound speed: This calculation repeats calculation (3) with higher compressional wave velocities in each layer. The new sound speeds correspond closer to logs from hole U8a10.^[1] To reach these higher velocities, each layer is given a larger bulk and shear modulus. However, its Poisson's ratio remains the same as for the corresponding layer of calculation (3). The higher sound speeds are

Layer 1 $C_o = 2.03$ km/sec (6700 ft/sec)

Layer 2 $C_o = 2.41$ km/sec (7900 ft/sec)

Layer 3 $C_o = 2.0$ km/sec (6600 ft/sec)

5. Constant Poisson's ratio: This calculation is identical to calculation (3) except that the shear modulus for each calculational zone is allowed to vary during porous crushup in order to maintain Poisson's ratio constant for that zone.

The results of this study are summarized in Table 4. Comparing calculations (1) and (1a), clearly the thickness of layer 2 is not a significant factor in magnitude of the peak residual stresses (note that all residual stresses are relative to an overburden pressure P_o of 60 bars), final cavity radius or pressure, or RDP. The RDP (or steady state value of the

Table 4
Results of Parameter Study

ID	Peak Transverse Residual Stress (bars)	Peak Radial Residual Stress (bars)	Cavity Radius (meters)	Cavity Pressure (bars)	RDP (m ³)
1	21.6	5.5	43.96	19.5	7350
1a	22.4	7.6	44.68	19.7	7600
2	62.2	25.2	44.57	18.3	7250
3	77.7	40.0	43.72	41.5	7800
4	73.2	35.9	43.77	41.4	7000
5	78.4	32.2	43.48	42.3	9800

reduced displacement potential) is defined as the final displacement multiplied by the square of the initial radial distance from the WP. It is a constant with position in the far (elastic) field and is a qualitative measure of the teleseismic coupling. It will be discussed later when Baneberry results are compared with calculations of events in other NTS media.

Calculation (2) shows that, for higher material strength, the residual stresses are increased dramatically. This is in agreement with the results of Rimer,^[5] which indicate that increasing Y_0 is most effective in increasing residual stress magnitudes. Cavity pressure is relatively unchanged.

When the cavity equation of state is altered as in calculation (3), a larger cavity pressure is noted, together with a smaller cavity radius. This larger cavity pressure is still somewhat smaller than overburden. Modifications in compressional wave velocity (calculation 4) or in elastic behavior (calculation (5)) have little effect.

This sensitivity study indicates that the residual stresses are primarily affected by changes in material strength while cavity pressure is modified by changes in the cavity equation of state. The basic results of Reference 4 remain unchanged. The residual stresses, while larger for the high strength calculations, are still much smaller than the results for Yucca Flat tuff and for Rainier Mesa tuff presented in Reference 4.

4. THE EFFECT OF CLAY AND WATER ON RESIDUAL STRESSES

Spherical, one-dimensional SKIPPER calculations for a working point medium having extremely high clay and water content (the Baneberry event) are discussed in this section and compared with calculations for Yucca Flat dry tuff and for the saturated tunnel tuffs of Rainier Mesa. All calculations use the same constitutive modeling and the same device yield so that differences in the results are a function only of the material properties chosen (constitutive models are discussed in detail in Section 2 and material properties for the calculations are given in Table 2). Table 5 shows the important results of these calculations.

The events considered for Rainier Mesa are Dido Queen in a weaker tunnel tuff environment and Mighty Epic in a stronger, atypical tunnel tuff. A second Dido Queen calculation was made for comparison using the Baneberry overburden pressure of 60 bars which barely perturbed the results. The Yucca Flat dry tuff calculations represent average properties for that area. These two Yucca Flat calculations differ only in the failure envelope used as do the two Baneberry calculations presented. All Baneberry calculations assumed 2 layers; one having greater than 50 percent montmorillonite clay, and the other less than 50 percent.

Table 5 gives the maximum values of the residual stresses in the radial and transverse (hoop) directions relative to the scalar overburden pressure. The Baneberry calculations showed much lower residual stresses when compared with the other Yucca Flat calculations. While the comparison with the weaker Rainier Mesa calculations (Dido Queen) was not as dramatic, the calculations still differ considerably. The most important material properties in determining the values of the residual stresses are the magnitude and shape of the failure surface. Since the "strong" Baneberry

Table 5
Comparison of Baneberry, Rainier Mesa, and Yucca Flat

Event	Peak Transverse Residual Stress (bars)	Peak Radial Residual Stress (bars)	Overburden (bars)	Cavity Radius (meters)	Cavity Pressure (bars)	RDP 3 (m)
Rainier Mesa						
Dido Queen 1	184	117	75	36.34	79.2	5000
Dido Queen 2	189	127	60	36.72	76.3	5700
Mighty Epic	588	319	75	26.54	207.7	950
Yucca Flat Dry Tuff						
1 (weak)	304	174	60	31.70	136.7	2500
2 (strong)	565	310	60	27.57	225.0	1400
Baneberry						
1 (strong)	132	76	60	40.45	53.1	5200
2 (weak)	77	46	60	44.34	38.5	8400

calculation uses a failure surface determined for Diagonal Line alluvium, recognized as a very strong, atypical alluvium, the "weak" calculation is probably a more believable estimate of the residual stresses around the Baneberry cavity.

The residual stresses must prevent the cavity pressure from hydrofracturing the surrounding rock. Table 5 shows cavity pressures obtained from the SKIPPER calculations. These cavity pressures are the least reliable part of the calculations since they are obtained using a simple bubble model described in Section 2 to initiate the explosion. Cavity radius is presented for each calculation at the same yield. Again, the most significant influence on cavity size is the failure envelope, higher strength giving smaller cavities and vice versa. There is a general trend of smaller cavities indicating higher cavity pressures.

A primitive measure of the teleseismic coupling implied by these calculations is given by the steady state value of the reduced displacement potential (RDP) shown for yields corresponding to Baneberry. Data compiled by Savino^[18] of S^3 show that both for regional and teleseismic measurements, Baneberry has the same body wave magnitude as Yucca Flat shots of 4 to 5 times the Baneberry yield. Also, for the same depth of burial, Baneberry has 4 or 5 times the surface wave amplitude. The data based on Bache, et al.^[19] therefore indicates that the average Yucca Flat calculation has the proper RDP relative to the best guess "weak" Baneberry calculation. (RDP varies linearly with yield.) Data from Savino also shows body wave magnitudes from Baneberry comparable to typical Rainier Mesa events. This tends to indicate that either Baneberry calculation would be satisfactory, with the "strong" being slightly preferred.

Other Baneberry calculations were made; one varying the magnitude of the yield strength in layer 1 (the high clay

content WP layer), and another the location of the interface between layers 1 and 2. These calculations showed that the strength and location of layer 1 had no influence on the peak residual stress which occurred in layer 2 for all calculations. The strength and location of layer 1 did influence cavity size and therefore cavity pressure.

Figures 2-7 show the complete residual stress fields for the calculations of Table 5 (Dido Queen 1 is not included since it is almost identical to Dido Queen 2). Note that the overburden pressure has not been subtracted out from these stresses. It is observed that higher strength not only increases the peak residual stress, it also makes the peak values occur closer to the WP. (This is partially a consequence of smaller cavity size.) For lower strengths, the stress field is spread out over a considerably greater volume, however. All the calculations considered the medium to be infinite in extent and, so, neglected free surface effect. However, the free surface will have the effect of reducing the magnitude of these residual stresses. For Baneberry, where the free surface is only 278 meters from the working point, well within the calculated residual stress field, the residual stress field would be greatly affected. Although these results cannot be considered definitive evidence, they are instructive and thought provoking. They strongly suggest that devices should be buried more deeply in a weaker medium.

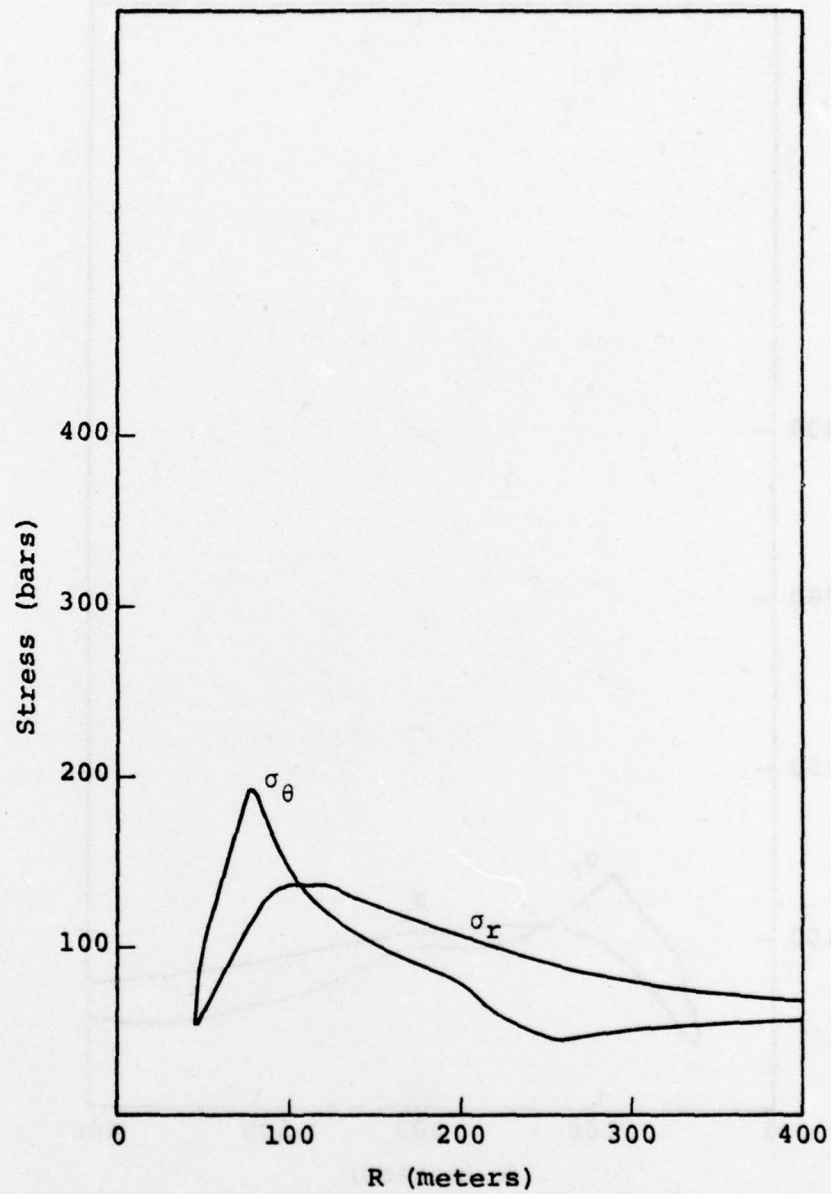


Figure 2. Residual stress field versus position for Baneberry 1 (strong).

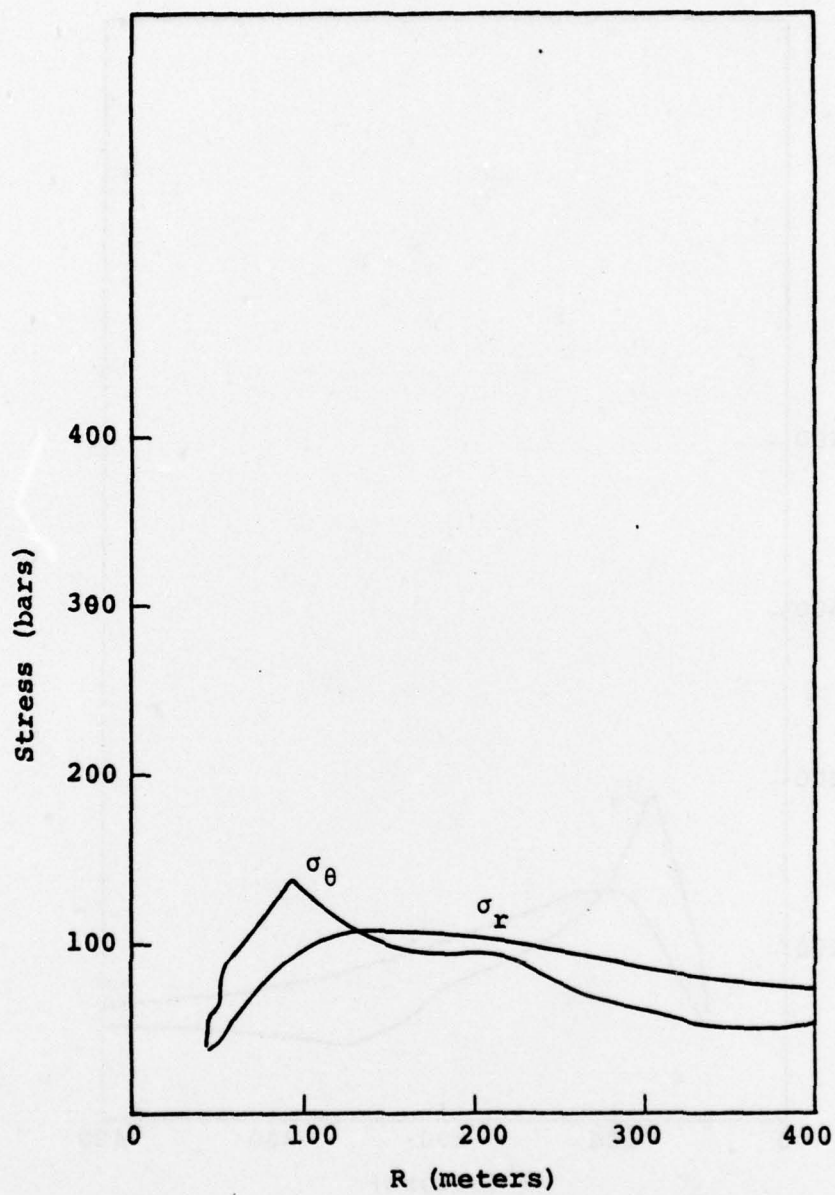


Figure 3. Residual stress field versus position for Baneberry 2 (weak).

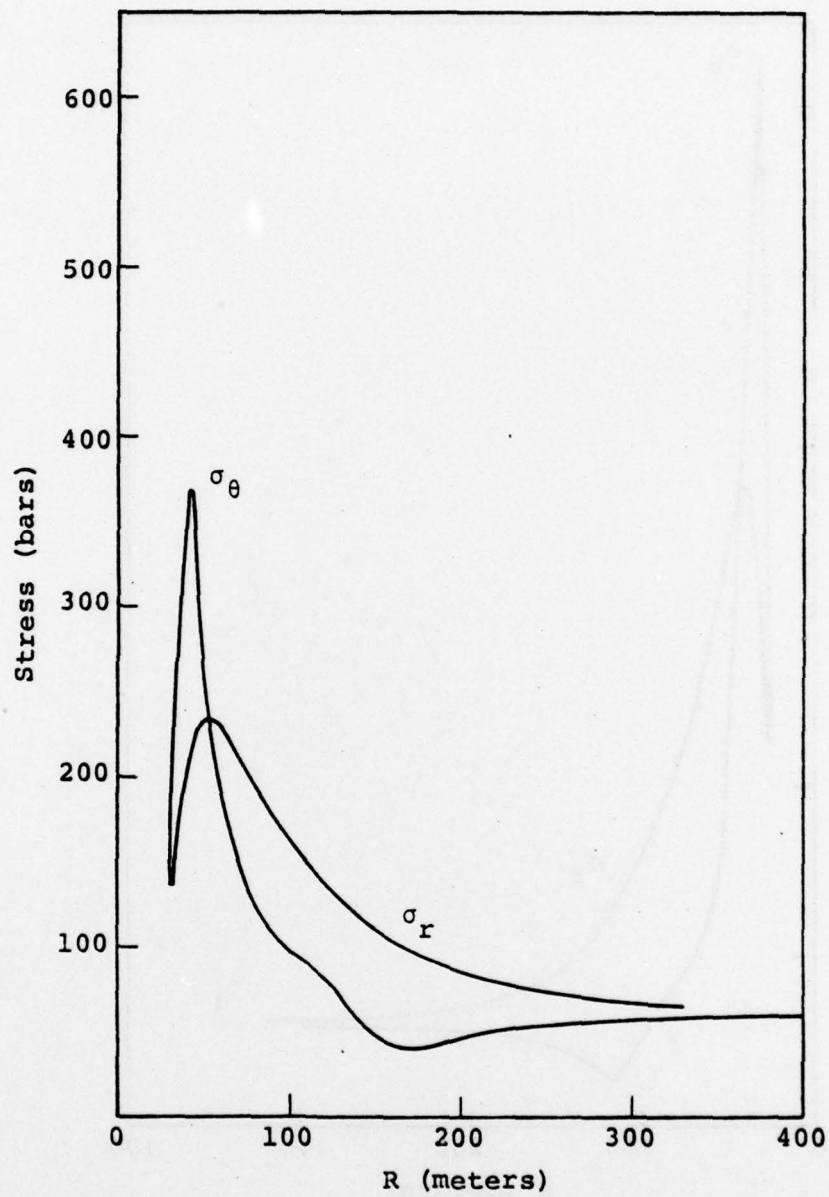


Figure 4. Residual stress field versus position for Yucca Flat 1 (weak).

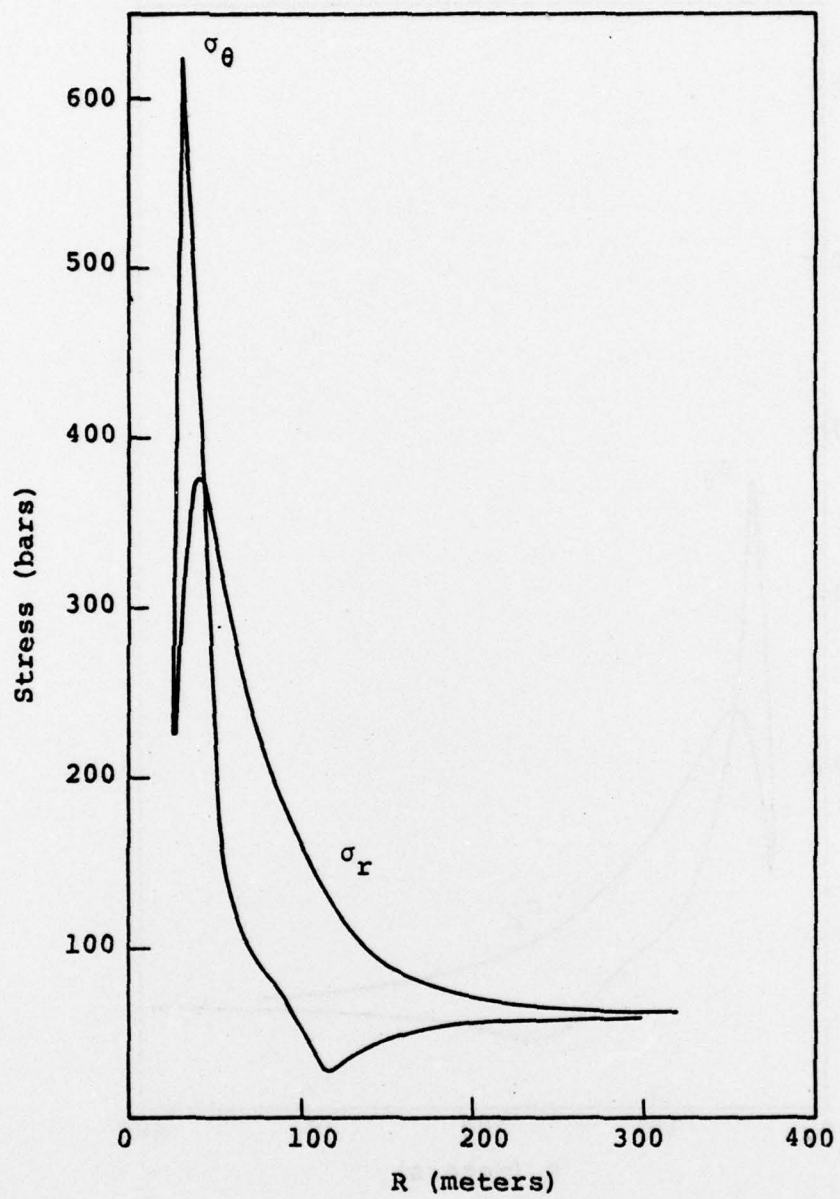


Figure 5. Residual stress field versus position for Yucca Flat 2 (strong).

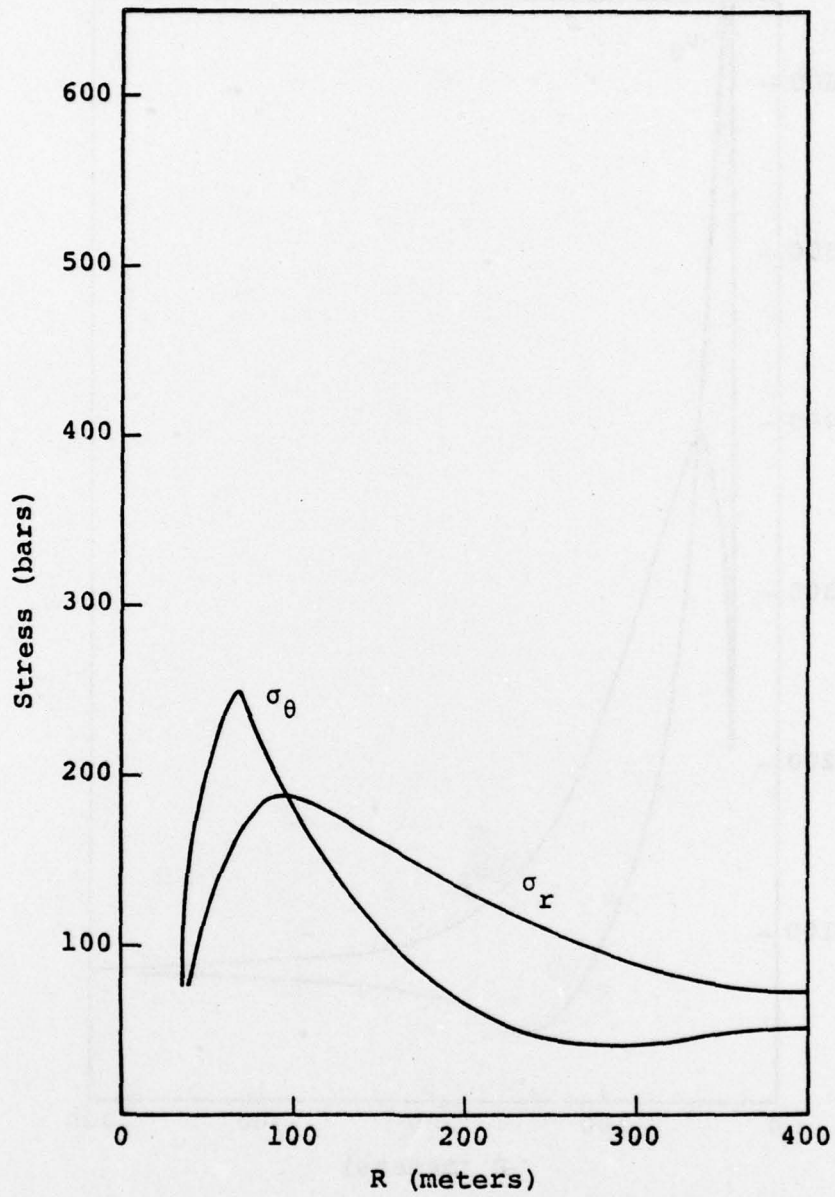


Figure 6. Residual stress field versus position for Dido Queen.

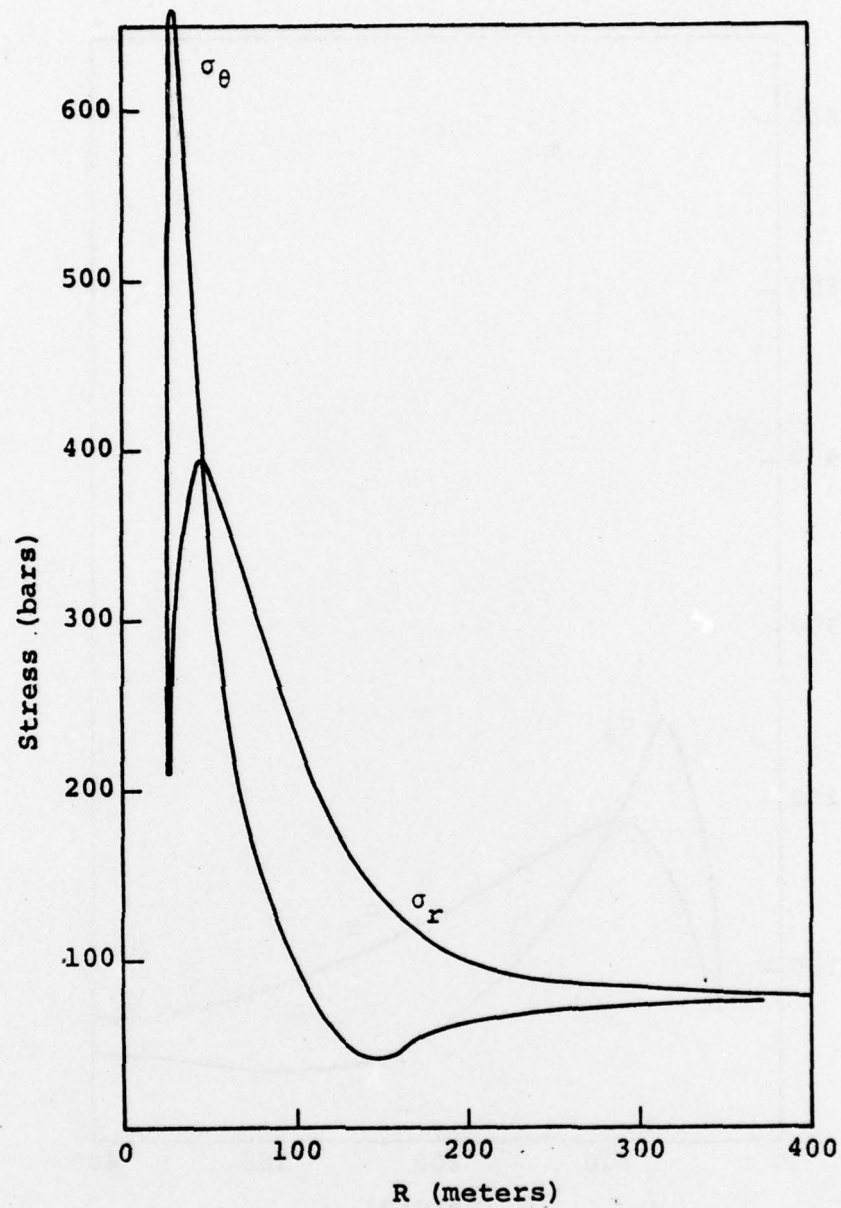


Figure 7. Residual stress field versus position for Mighty Epic.

5. FIGURES OF MERIT

It is difficult to quantify what is important to containment of the cavity gases when comparing the calculations of Table 5 (Section 4). Some possible "figures of merit" are discussed in this section. In Reference 4, and in Section 4 of this report, the values of the peak residual stresses (particularly the hoop stresses), relative to the scalar overburden pressure, were compared. It is reasonable to use the stresses with the overburden subtracted out as a measure of containment since the philosophy is that it is the additional stresses over the overburden which forms the containment membrane to prevent hydrofracture from the cavity. There it was stated that containment was better when the peak residual stresses were higher.

This simple figure of merit does not give the complete picture, however. Figures 2-7 show that the residual stress fields look quite different for strong media (where the peak stresses are high) and weak media. For weak media, the compressive hoop stresses, though smaller in magnitude, tend to occur over a larger radial distance, i.e., the residual stress membrane is thicker. However, we believe that a thinner, but significantly higher stress membrane is far more effective as a containment membrane, so that we will continue to use the peak residual stress in our figure of merit.

Of course, these residual stresses must resist a cavity pressure. Based on the simple mechanics of materials problem of a thin walled pressure vessel, the ratio of cavity pressure to peak transverse residual stress would appear to be a reasonable figure of merit. However, the cavity pressure computed using SKIPPER is not a good measure of the real cavity pressure. It takes no account of water getting into the cavity from the surrounding rock or of additional thermal equilibration expected in the rock outside the calculated

cavity. A procedure developed by Peterson and Lie^[20] to obtain cavity pressures and temperatures for cavity leak calculations was modified here and used to calculate a better value of cavity pressure from the output of the SKIPPER calculations.

Starting from the final state obtained from the SKIPPER output (cavity radius, cavity energy, internal energy and mass of adjacent zones, etc.) and beginning at the cavity boundary, small amounts of mass of rock (and its accompanying internal energy) are equilibrated with the melted cavity material which is at a specific internal energy greater than the melt energy of the rock. This calculational procedure approximates the physical processes of spall and equilibration. The process is stopped when sufficient mass has been added so that the equilibrated "cavity" is at the melt energy. Finally, the volume of steam in the new cavity is computed based on the water content of the undisturbed rock, and a final cavity pressure is calculated (for the steam).

One question which arises involves how much water is in the undisturbed rock. The water content by weight, f_w , given in Table 2 of Section 2, is defined as the amount of water that can be removed at 105°C. This does not include the bound water in the rock. For Rainier Mesa tuff, this amounts to approximately 7 percent extra water by weight.^[20] The cavity pressure was computed for each of the calculations shown in Table 5, using f_w alone and also including the additional bound water (assumed to be 7 percent for all media). Table 6 presents the results of these computations. Note that the effect of equilibrating the cavity with the outside material is to reduce the cavity pressure for all cases. When the bound water is included in the computation of cavity pressure, less of a change results, as would be expected. (The mass of rock material reduces the pressure while the water tends to increase it.)

Table 6
Figures of Merit for Equilibrated and Unequilibrated Cavities

Event	f_w	Peak Transverse Residual Stress σ_t (bars)	Equili- brated Cavity Radius (meters)	Unequili- brated Cavity Pressure, P_1 (bars)	Equilibrated Cavity Pressure (bars)			Figures of Merit		
					No Bound Water P_2	Bound Water P_3		$\frac{P_1}{\sigma_t}$	$\frac{P_2}{\sigma_t}$	$\frac{P_3}{\sigma_t}$
Rainier Mesa										
Dido Queen 1	0.16	184	36.70	79.3	39.4	55.4		0.43	0.21	0.30
Dido Queen 2	0.16	189	37.09	76.3	36.5	54.9		0.40	0.19	0.29
Mighty Epic	0.17	588	27.40	207.7	101.4	147.6		0.35	0.17	0.25
Yucca Flat Dry Tuff										
1 (weak)	0.13	304	32.18	136.7	51.8	84.1		0.45	0.17	0.27
2 (strong)	0.13	565	28.35	225.0	95.4	152.2		0.40	0.17	0.27
Baneberry										
1 (strong)	0.22	132	40.62	53.1	34.6	47.1		0.40	0.26	0.36
2 (weak)	0.22	77	44.49	38.5	24.0	32.4		0.50	0.31	0.42

Here, σ_t is the peak transverse residual stress and the figures of merit chosen are ratios of the calculated cavity pressures, P_1 , P_2 and P_3 to σ_t . Let us define a higher ratio of cavity pressure to σ_t as a greater relative containment risk. For both the figures of merit in which cavity pressure from an equilibrated cavity was used, both Baneberry calculations are clearly less conservative and therefore relatively greater containment risks. Using the unequilibrated cavity pressure, the "weak", best guess, Baneberry 2 calculation is the worst risk. However, the "strong" Baneberry 1 calculation lies within the data for the other events.

Summarizing, for all figures of merit investigated, the "best guess" Baneberry 2 calculation is clearly the worst risk. Only when the unequilibrated cavity pressure (a hardly justifiable choice) is used, does even the strong upper limit Baneberry 1 calculation appear as safe as for other events.

REFERENCES

1. U. S. Geological Survey Report, "Results of Exploration of Baneberry Site, Early 1971," USGS-474-145, July 1974.
2. Ramspott, L. D., private communication, Lawrence Livermore Laboratory, 1975.
3. Butters, S. W., Terra Tek, letter to Mr. Carl Keller, DNA Field Command, May 25, 1976.
4. Rimer, N., "A Scenario for the Containment Failure of Baneberry," Systems, Science and Software Topical Report SSS-R-75-2703, August 1975.
5. Rimer, N., "The Relationship Between Material Properties, Residual Stresses, and Cavity Radius Due to a Nuclear Explosion," Systems, Science and Software Topical Report SSS-R-76-2907, May 1976.
6. Cherry, J. T., N. Rimer and W. O. Wray, "Seismic Coupling from a Nuclear Explosion: The Dependence of the Reduced Displacement Potential on the Nonlinear Behavior of the Near Source Rock Environment," Systems, Science and Software Report SSS-R-76-2742, September 1975.
7. Tillotson, J. H., "Metallic Equations of State for Hypervelocity Impact," General Atomic Report GA-3216, July 1962.
8. Cherry, J. T. and F. I. Peterson, "Numerical Simulation of Stress Wave Propagation from Underground Nuclear Explosions," Engineering with Nuclear Explosives, ANS, USAEC, Conf. 700101, 1970.
9. Maenchen, G. and S. Sack, "The TENSOR Code," in Methods in Computational Physics, Vol. 3, Academic Press, New York, 1964.
10. Laird, D. H., "A Chemical Equilibrium Equation of State for Saturated Tuff," Systems, Science and Software Topical Report SSS-R-75-2740, January 1976.
11. Stephens, D. R., H. C. Heard and R. N. Schock, "Preliminary Equation of State Data for Baneberry Altered Tuff," Lawrence Livermore Laboratory Memorandum UCID-15874, July 13, 1971.

12. Butters, S. W., R. J. Reid, S. J. Green and A. H. Jones, "Mechanical Properties of Nevada Test Site Tuff from Selected Exploratory Drill Holes," Terra Tek, Inc. Final Report TR 73-28, July 1973.
13. Rimer, N., R. Herrmann and R. Duff, "A Calculation of the Interface Motion from the Mighty Epic Event," Systems, Science and Software Topical Report SSS-CR-77-3056, November 1976.
14. Ramspott, L. D. and N. W. Howard, "Average Properties of Nuclear Test Areas and Media at the USERDA Nevada Test Site," Lawrence Livermore Laboratory Report UCRL-51948, September 15, 1975.
15. App, F. N., Los Alamos Scientific Laboratory, letter to Dr. Russell Duff, Systems, Science and Software, June 7, 1976.
16. Heard, H. C. and D. R. Stephens, "Compressibility and Strength Behavior for Diagonal Line Alluvium," Lawrence Radiation Laboratory Report UCID-15736, October 14, 1970.
17. Bonner, B. P., A. E. Abey, H. C. Heard and R. N. Schock, "High-Pressure Mechanical Properties of Merlin Alluvium," Lawrence Livermore Laboratory Report UCRL-51252, July 7, 1972.
18. Savino, J., private communication, April 1977.
19. Bache, T. C., T. G. Barker, N. Rimer, T. R. Blake, D. G. Lambert, J. T. Cherry and J. M. Savino, "An Explanation of the Relative Amplitudes of the Teleseismic Body Waves Generated by Explosions in Different Test Areas at NTS," Systems, Science and Software Final Report DNA 3958F, October 1975.
20. Peterson, E. W. and K. Lie, "Hudson Moon Leak Evaluation," Systems, Science and Software Topical Report (in preparation).

DISTRIBUTION LIST

DEPARTMENT OF DEFENSE

Defense Documentation Center
Cameron Station
12 cy ATTN: TC

Director
Defense Nuclear Agency
ATTN: DDST
ATTN: TISI
3 cy ATTN: TITL

Commander
Field Command
Defense Nuclear Agency
ATTN: FCPR
ATTN: FCTMC, Carl Keller

Director of Defense Research & Engineering
Department of Defense
ATTN: S&SS (OS)

Chief
Livermore Division, Field Command, DNA
Lawrence Livermore Laboratory
ATTN: FCPRL

Chief
Test Construction Division
Field Command Test Directorate
Defense Nuclear Agency
ATTN: NTS, Joe LaComb

DEPARTMENT OF THE ARMY

Commander
Harry Diamond Laboratories
ATTN: DRXDO-NP

DEPARTMENT OF THE NAVY

Officer-in-Charge
Naval Surface Weapons Center
ATTN: Code WA501, Navy Nuc. Prgms. Off.

DEPARTMENT OF THE AIR FORCE

AF Weapons Laboratory
ATTN: SUL

ENERGY RESEARCH & DEVELOPMENT ADMINISTRATION

University of California
Lawrence Livermore Laboratory
ATTN: David Oakley
ATTN: Billy Hudson
ATTN: Mr. Terhune

ENERGY RESEARCH & DEVELOPMENT ADMINISTRATION (Continued)

Los Alamos Scientific Laboratory
ATTN: Robert Brownlee
ATTN: Fred App

Sandia Laboratories
ATTN: Wendell Weart/Lynn Tyler

US Energy Research & Development Admin.
Nevada Operations Office
ATTN: Robert Newman

OTHER GOVERNMENT AGENCY

Department of Commerce
US Geological Survey
Special Projects Branch
ATTN: Rod Carroll

DEPARTMENT OF DEFENSE CONTRACTORS

Pacifica Technology
ATTN: G. I. Kent

Physics International Company
ATTN: E. T. Moore

SRI International
ATTN: Alex Florence

Systems, Science & Software, Incorporated
ATTN: Russell E. Duff
ATTN: Norton Rimer

Terra Tek, Incorporated
ATTN: Sidney Green

General Electric Company
TEMPO-Center for Advanced Studies
ATTN: DASIAC